Mathematical Models and Methods in Applied Sciences

Energy minimizing twinning with variable volume fraction, for two nonlinear elastic phases with a single rank-one connection

Sergio Conti

Institut für Angewandte Mathematik, Universität Bonn, 53115 Bonn, Germany
sergio.conti@uni-bonn.de

Robert V. Kohn

Courant Institute, New York University, New York, NY, 10012, USA
kohn@cims.nyu.edu

Oleksandr Misiats

Department of Mathematics and Applied Mathematics, Virginia Commonwealth University, Richmond, VA, 23284, USA
omisiats@vcu.edu

Received (Day Month Year)
Revised (Day Month Year)
Communicated by (xxxxxxxxxx)

In materials that undergo martensitic phase transformation, distinct elastic phases often form layered microstructures – a phenomenon known as twinning. In some settings the volume fractions of the phases vary macroscopically; this has been seen, in particular, in experiments involving the bending of a bar. We study a 2D model problem of this type, involving two geometrically nonlinear phases with a single rank-one connection. We adopt a variational perspective, focusing on the minimization of elastic plus surface energy. To get started, we show that twinning with variable volume fraction must occur when bending is imposed by a Dirichlet-type boundary condition. We then turn to paper's main goal, which is to determine how the minimum energy scales with respect to the surface energy density and the transformation strain. Our analysis combines ansatz-based upper bounds with ansatz-free lower bounds. For the upper bounds we consider two very different candidates for the microstructure: one that involves self-similar refinement of its length scale near the boundary, and another based on piecewise-linear approximation with a single length scale. Our lower bounds adapt methods previously introduced by Chan and Conti to address a problem involving twinning with constant volume fraction. The energy minimization problem considered in this paper is not intended to model twinning with variable volume fraction involving two martensite variants; rather, it provides a convenient starting point for the development of a mathematical toolkit for the study of twinning with variable volume fraction.

Keywords: Solid-solid phase transitions; twinning; nonlinear elasticity.

AMS Subject Classification: 74N15, 49J35, 74B20

1. Introduction

Martensitic phase transformation of a crystalline solid leads to the formation of elastic domains. The associated pattern formation problems have been studied by many authors, using a variety of methods including the crystallographic theory of martensite, phase-field-type numerical algorithms, and variational approaches involving minimization of elastic energy or elastic plus surface energy. This paper is motivated by the variational perspective.

It often occurs that two phases form a layered microstructure – a phenomenon known as twinning (see for example Refs. 1, 4, 19, 29). Problems involving twinning with constant volume fraction have received a lot of attention over the years. The length scale of twinning near an austenite interface has been a particular focus of research (see Ref. 12 for some recent developments and references to prior work). Interestingly, in that setting the length scale of twinning can be very nonuniform – small where the twins meet the austenite, but much larger at points far from this interface. The change of length scale is accomplished by branching, which is predicted (at least by one model[11]) to be self-similar.

In this paper we study a similar yet different microstructure – one we like to call "twinning with variable volume fraction" – which has thus far received much less attention. As we shall see, the situation is quite different from – though it has connections to – twinning at constant volume fraction.

Why might the volume fraction vary macroscopically? We focus in this paper on a simple two-dimensional thought-experiment involving the bending of a bar (see Figure 1). We introduce it informally here, then more mathematically in Section 2.1. The bar is initially rectangular (with long direction parallel to the y axis), occupied entirely by one of our two elastic phases. Suppose the transformation strain taking this phase to the other one expands the y direction but leaves the x direction invariant. Then bending the bar should create a two-phase mixture to accommodate the required expansion without substantial elastic energy, as shown on the right hand side of Figure 1. While this thought-experiment is somewhat stylized, it captures many features of some real-world examples, as we shall explain in Section 2.6.

This paper studies the minimization of elastic plus surface energy, for a mathematical model of this thought-experiment. The bending is imposed not by forces, but rather by a suitable Dirichlet-type boundary condition. Since the variational problem being considered is highly nonconvex, it is unreasonable to expect to identify the exact energy minimizer either analytically or numerically. Instead, we focus on understanding the *energy scaling law* – that is, how the minimum energy scales with respect to the surface energy coefficient and the transformation strain. Upper bounds come from specific test functions, which are built around candidate two-phase geometries. One of our upper bounds is built around the geometry shown in Figure 1; another uses self-similar branching to make the length scale of the microstructure near the curved boundaries much smaller than in the center. To identify the energy scaling law, one must prove an ansatz-free lower bound that

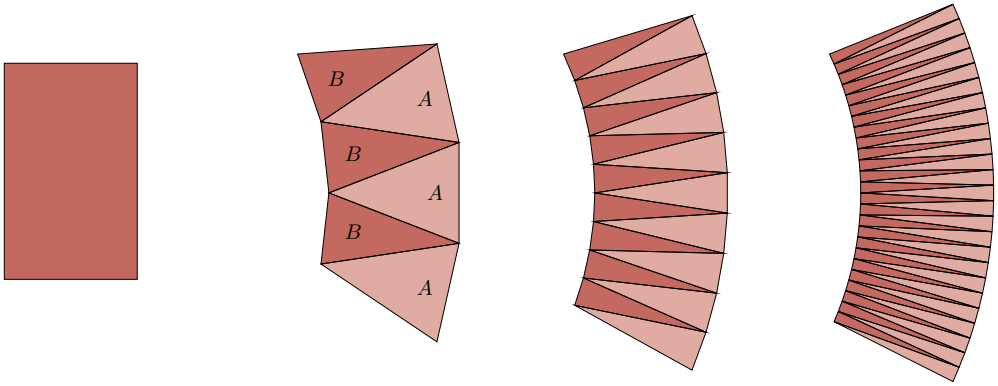

Fig. 1. Explanation why bending of a bar leads to twinning with variable volume fraction. The two phases are dark (B) and light (A) respectively. LEFT: the unbent bar (short in the x direction and long in the y direction) is entirely in the dark phase (though an unbent bar could also be a mixture of the two phases, in twins parallel to the x axis). RIGHT: if transformation from the dark phase to the light phase expands the material in the y direction, then the bent bar can keep its elastic energy small by using a piecewise affine mixture of the two phases with one phase dominating on the left and the other dominating on the right. The sequence of pictures shows how refinement of the microstructure leads to a better approximation of the relaxed solution u^* in (1.3) and of the chosen boundary conditions, at the expense of higher surface energy. The optimal length scale depends on the cost of interfaces and is therefore material dependent. The construction used to prove Lemma 3.1 is based on this picture. Since the deformation associated with this picture is piecewise affine, the bent structure it achieves has a polygonal boundary. To make the left and right boundaries exactly pieces of circles a somewhat different construction is needed, in which the length scale of the twinning approaches zero near the left and right edges. Lemma 3.5 uses a branching pattern to achieve this.

scales the same way as the upper bound. When this program is successful – as happens here – the impact of the lower bound is two-fold: on the one hand it confirms the near-optimality of a configuration achieving the upper bound; and on the other hand, the proof of the lower bound provides an *explanation* why no configuration can do much better.

The preceding paragraph and Figure 1 provide an equation-free summary of our goals. Section 2.1 explains in detail the variational problem we consider. An impatient (and sufficiently expert) reader might, however, appreciate the following summary of our setting. Working in two spatial dimensions, we assume that there are two variants of martensite, characterized by the eigenstrains

$$A := \begin{pmatrix} 1 & 0 \\ 0 & 1+\alpha \end{pmatrix} \qquad \text{and} \qquad B := \begin{pmatrix} 1 & 0 \\ 0 & 1-\alpha \end{pmatrix}, \tag{1.1}$$

where $\alpha \in (0, \frac{1}{2}]$ is a parameter. Obviously $\frac{1}{2}(A+B) = \mathrm{Id}$. The elastic energy measures the distance of the deformation gradient from the set $K = \mathrm{SO}(2)A \cup \mathrm{SO}(2)B$, see (2.1)–(2.5) for details. The matrices A and B are rank-one connected, with $\mathrm{rank}(A - QB) = 1$ having a single solution at $Q = \mathrm{Id}$. The quasiconvex

envelope of K turns out to be

$$K^{\mathrm{qc}} = \{Q(tA + (1-t)B) : t \in [0,1], Q \in \mathrm{SO}(2)\} \tag{1.2}$$

(see Lemma 2.1). It is natural to interpret the parameter t in (1.2) as the local volume fraction of the variant A, with $1-t$ being the local volume fraction of the variant B. We choose a prototypical deformation u^* with $Du^* \in K^{\mathrm{qc}}$, and with volume fraction depending on position, of the form

$$u^*(x,y) := \frac{1+\alpha x}{\alpha} \begin{pmatrix} \cos(\alpha y) \\ \sin(\alpha y) \end{pmatrix} \tag{1.3}$$

for $(x,y) \in (-1,1) \times \mathbb{R}$. One can check that the deformations illustrated in Figure 1 would converge, as the microstructure becomes finer, to u^* (weakly in $W^{1,2}_{\mathrm{loc}}((-1,1)\times \mathbb{R}; \mathbb{R}^2)$). A short computation shows that

$$Du^*(x,y) = Q_{\alpha y}\left(\frac{1+x}{2}A + \frac{1-x}{2}B\right) \in K^{\mathrm{qc}} \tag{1.4}$$

pointwise, showing that the local volume fraction of the A variant is $\frac{1+x}{2}$. Here $Q_{\alpha y} \in \mathrm{SO}(2)$ is a rotation, defined in (3.4) below. It turns out that u^* is the only minimizer of the relaxed problem if we prescribe Dirichlet boundary conditions on the vertical sides, $x = \pm 1$, see Lemma 2.2. Therefore approximate solutions of the unrelaxed problem with these boundary conditions converge to u^*, and the volume fraction of the two phases converges to the ones obtained for u^*.

The variational problem we consider is then to minimize an *unrelaxed* elastic energy, of the form $\mathrm{dist}^2(Du, K)$, plus a singular perturbation proportional to the total variation of Du, subject to the condition that $u = u^*$ for $x = \pm 1$, see (2.8)–(2.9). In the limit of small surface energy ε, minimizers u_ε converge to u^*, and therefore locally the volume fraction of the A phase approximates $\frac{1+x}{2}$. With reference to the deformations shown in Figure 1, we remark that for any finite length scale $h > 0$ the A/B interfaces are not parallel to the B/A interfaces. Indeed, this is a necessary consequence of the fact that the volume fractions depend on x. Since the interfaces deviate from the rank-one direction, the elastic energy cannot vanish, even if the boundary conditions are satisfied only approximately. However, the slope of the interfaces depends on h, which in turn relates to the surface energy. We refer to Remark 2.2 for a brief discussion of the relevant scalings, and to the upper bounds in Section 3 for a detailed computation. Therefore in the current problem a competition between elastic and surface energy is present for any map that approximates u^*, and does not depend on the detailed boundary conditions.

Our main results are stated in Section 2.5, but let us summarize them informally here:

(a) We evaluate the energy scaling obtained using a piecewise linear test function with the phase geometry shown in Figure 1. We also evaluate the energy scaling obtained using a construction involving self-similar branching of the elastic domains. The two constructions achieve the same energy scaling law. Their

boundary behavior is slightly different: the self-similar construction achieves our "bending boundary condition" exactly (the deformed rectangle occupies a sector of an annulus) while the unrefined piecewise linear construction achieves it only approximately (the deformed rectangle occupies a piecewise linear approxmation of an annulus).

(b) We prove an ansatz-free lower bound, showing that the energy scaling law achieved by these two constructions is optimal.

(c) We consider whether a construction similar to Figure 1 can be adapted to achieve our bending boundary condition exactly (mapping the deformed rectangle to a sector of an annulus) without changing its energy scaling law. The answer is no. In fact, the obvious adaptation – an interpolation near the edges – achieves a different scaling law. Moreover we prove a lower bound showing that this different scaling law is optimal among constructions whose local length scale near the boundary is similar to that in the interior. Thus, while the details of our self-similar construction are surely not unique, achievement of the exact bending boundary condition seems to require something of this sort.

Item (a) summarizes the upper-bound parts of Theorems 2.1 and 2.2; (b) summarizes the lower-bound parts of the same theorems; and (c) summarizes Theorem 2.3.

It might seem surprising that the unrefined construction and the one with self-similar branching lead to the same scaling of the energy. This is quite different from situation for twinning with constant volume fraction, as considered for example in Refs. 21, 22, 23. To explain why branching doesn't change our energy scaling law, it is useful to point out that in the branching construction the total energy is estimated (much as in the papers just cited and other work on similar patterns discussed in Section 2.6 below) by a converging geometric series (see (3.47)). The scaling behavior is therefore controlled by the first term of the series, which decribes the bulk behavior. In our setting, the behavior in the bulk involves both elastic and surface energy. (The elastic energy is inescapable since the volume fractions are position-dependent – a feature that's present whether or not one uses branching.) This is quite different from the situation with constant volume fraction, where the unrefined construction has zero elastic energy in the bulk. This is, we believe, the essential reason why the two constructions lead to the same scaling.

As we have just summarized, our paper presents two rather different constructions with the same energy scaling law. One may wonder which is more likely to be observed in practice. Within the variational setting, one would have to compare the energy of the two constructions, which would require understanding the prefactor in the energy scaling, and is beyond the scope of the present paper. It seems natural to expect that the simplest pattern will have a smaller prefactor, but one should keep in mind that many other patterns are also possible, for example with partial branching. However, energy minimization alone cannot predict what is observed in nature, and indeed it is known that experiments in the presence of highly nonconvex energies are typically not fully described by energy minimization. In practice, devel-

opment of microstructure strongly depends on nucleation phenomena. Whereas it seems natural to think that the simpler, unrefined structure might be preferred, the precise answer may depend on other details of the problem not modeled here, and be history-dependent. We stress that the advantage of branching obtained in item (c) above stems from the idealized rigid boundary conditions. Although the fact that the volume fraction depends on position seems robust in this setting, the appearance of branching might be due to the specific Dirichlet boundary data chosen here.

Concerning methods: in the limit as the surface energy density tends to zero, the energy minimizer must converge (weakly in H^1) to the minimizer of a suitable "relaxed problem" involving the quasiconvexification of the elastic energy. Therefore our analysis begins with a discussion of the relaxed problem (Lemmas 2.1 and 2.2). We then turn, in Section 3, to the constructions that give our upper bounds. The piecewise linear test function motivated by Figure 1 resembles one that was briefly discussed in an analogous scalar setting in Ref. 25. The test function involving self-similar branching is conceptually similar to those previously used to model twinning with constant volume fraction near an austenite interface; we draw ideas especially from the work of Chan and Conti[5,6], which uses geometrically nonlinear elasticity (as we do here). However the details are quite different in the present variable-volume-fraction setting; therefore we present the self-similarly branched construction in full detail. Our lower bounds are presented in Section 4. The bounds mentioned in item (b) above are proved by adapting arguments from Refs. 5, 6 to our variable-volume-fraction setting. For those mentioned in item (c) above, even the statement of the theorem requires a new idea. Indeed, we need to formalize what it means for a test function to "have no microstructure near the boundary" (that is, to have its local length scale near the boundary similar to that in the interior). This is done by defining what it means to "have no microstructure on a set ω with constant m" (Definition 2.1), then using it to define a class of deformations $S^{(m)}_{\text{onescale}}$ that have, in a very precise sense, no microstructure near the boundary (Definition 2.2). Besides the definitions just discussed, the proof of the lower bound summarized by item (c) uses the Friesecke-James-Müller rigidity theorem, and a straightforward estimate of how well our bending boundary condition can be approximated by a piecewise linear function.

Two papers closely related to this work are in preparation. The paper in Ref. 24 considers twinning with variable volume fraction in the context of the scalar model briefly discussed in Ref. 25 (a variant of the scalar model introduced by Kohn and Müller[21,22,23] to study the length scale of twinning near an austenite-twinned-martensite interface). The analysis in Ref. 24 goes beyond the energy scaling law, using well-chosen comparison functions to draw conclusions about the geometrical character of an energy minimizer. In a different direction, the paper in Ref. 13 examines a 3D linear elastic model of the bending of a bar consisting of two martensite variants. The model considered there is basically a quantitative version of those in Refs. 7, 31; in particular, the transformation strain considered there is appropriate

for variants created by a cubic–tetragonal phase transformation. (Subsequent experimental work[8] by the authors of Ref. 7 reported that their bars had microstructures more complex than anticipated by the models in Refs. 7, 13, 31; in fact bending produced "polydomain phases," specifically a type of microstructure known in the mathematical literature as a "order-two laminate." Such microstructures have also recently been observed in another system.[9] It remains an interesting open problem to understand these bending-induced order-two laminates as minimizers of an appropriate energy functional.)

2. Mathematical formulation, main results, and scientific context

2.1. *Our variational problem*

The spatial arrangements of phases in systems undergoing coherent phase transformation have long been studied using the minimization of elastic energy, with or without surface energy; see e.g. Refs. 19, 29 for early work using geometrically linear elasticity, Refs. 1, 2 for early work using geometrically nonlinear elasticity, and Ref. 21 for early work about the effect of surface energy. In this paper we use a geometrically nonlinear elastic energy, and a formulation permitting sharp interfaces for the surface energy. Our variational problem is among the ones studied in Refs. 5, 6, though our boundary condition is different. Here and throughout the paper (except for Section 2.2), we discuss the problem in its nondimensional form. (The nondimensionalization is briefly discussed in Section 2.2.)

Our elastic energy: In a geometrically nonlinear theory, the elastic energy should have the form

$$\int_\Omega W(Du)\, d\mathcal{L}^n, \tag{2.1}$$

where W is frame-indifferent in the sense that $W(F) = W(RF)$ for every orientation-preserving rotation R. Here we work in space dimension two, with a special "two-well" elastic energy density of the form

$$W(F) = \mathrm{dist}^2(F, K) = \inf\{|F - G|^2, G \in K\}. \tag{2.2}$$

The set K (which represents the material's stress-free states) has the form

$$K = \mathrm{SO}(2)A \cup \mathrm{SO}(2)B \tag{2.3}$$

with

$$A := \begin{pmatrix} 1 & 0 \\ 0 & 1+\alpha \end{pmatrix}, \qquad B := \begin{pmatrix} 1 & 0 \\ 0 & 1-\alpha \end{pmatrix}, \tag{2.4}$$

where α is a parameter satisfying

$$0 < \alpha \le 1/2. \tag{2.5}$$

(The upper bound serves to keep us away from the singular case $\alpha = 1$.)

As usual in nonlinear elasticity, the elastic deformation u takes a reference domain Ω to a deformed configuration $u(\Omega)$. We shall focus on the reference domain

$$\Omega = (-1, 1) \times (-1, 1) \tag{2.6}$$

though we briefly comment on rectangular domains in Section 2.2.

Our elastic energy density (2.2) describes a two-phase elastic material. The stress-free strains of the two phases are A and B, and the Hooke's law of each phase is the identity. The choice of such a simple Hooke's law is, however, not essential. Indeed, since our results concern only the energy scaling law (not the prefactor associated with this law), they apply to any elastic energy density that is bounded above and below by a constant times our W.

Experts will notice that our two-well energy is *different* from those that typically arise in connection with shape-memory materials (see e.g. Ref. 4). Indeed, for an energy density of the form (2.2) with $K = \mathrm{SO}(2)A' \cup \mathrm{SO}(2)B'$ for two symmetric matrices A' and B' with $B' \notin \mathrm{SO}(2)A'$, there are three different cases:

(i) If $RA' - B'$ has rank 2 for every $R \in \mathrm{SO}(2)$, then the two phases cannot coexist in their stress-free states.
(ii) If $RA' - B'$ has rank 1 for a unique $R \in \mathrm{SO}(2)$, then the two phases can "twin" (that is, they can mix in layers in their stress-free states) in just one way. In fact, if $RA' - B' = a \otimes n$, then stress-free twinning uses layers normal to n.
(iii) If $RA' - B'$ has rank 1 for two distinct choices of $R \in \mathrm{SO}(2)$ then the two phases can twin in two different ways. In fact, if $R_1A' - B' = a_1 \otimes n_1$ and $R_2A' - B' = a_2 \otimes n_2$, then stress-free twinning can use either layers normal to n_1 or layers normal to n_2.

Our elastic energy density is typical of case (ii), while a pair of low-temperature variants in a shape-memory material would be in case (iii). We have chosen to focus on (ii) because it is the simplest nonlinear setting where the phenomenology captured by Figure 1 can be discussed. Our upper bound constructions have analogues in the setting of case (iii) (though the associated scaling laws are different from those of the present paper, reflecting differences between the two cases that are well-understood in the constant-volume fraction setting[5,6]). With respect to lower bounds, however, the situation in case (iii) seems quite different from that of the present paper, since there are stress-free mixtures of the two phases that achieve something like bending without any need for microstructure (see Ref. 17 for an up-to-date discussion with references to earlier work). It would, of course, be interesting to understand case (iii) better. The paper in Ref. 13 takes a step in this direction, by using geometrically linear elasticity to model the bending of a three dimensional bar made from a two-phase material to which (iii) applies.

Our surface energy: Our upper bound constructions use continuous, piecewise smooth deformations u. In the smooth parts Du is close to either $\mathrm{SO}(2)A$ or $\mathrm{SO}(2)B$, making the elastic energy small; where u is not smooth, it is because Du jumps

across a curve that can be thought of as a phase boundary. In a physical setting, the surface energy might have a complicated dependence on the orientation of the phase boundary and the deformation gradients on each side. But since we focus only on the scaling law of the minimum energy (not the prefactor), it is sufficient to use a simpler model: we require that Du be a (matrix-valued) BV function, we take the surface energy to be a multiple of its total variation:

$$\varepsilon |D^2 u|(\Omega) \tag{2.7}$$

(Here and throughout the paper, our norm on the space of matrices is the Euclidean one: $|F| := (\sum_{ij} F_{ij}^2)^{1/2}$.) The coefficient $\varepsilon > 0$ is a parameter. For stress-free twins, Du would take the values RA and RB in layers parallel to the x axis, and the surface energy would be $2\alpha\varepsilon$ times the arclength of the phase boundary. Thus the surface energy density is not ε, but rather $2\alpha\varepsilon$.

Our bending boundary condition: Figure 1 visualized the bending of a rectangle. However, the bending of a square $\Omega = (-1, 1)^2$ captures all the problem's essential mathematical issues, so we shall focus on this case (except in Section 2.2). We further specialize to the case when the deformed square has pure phase A on the right edge and pure phase B at the left edge (like Figure 1). The deformed square is then a sector of an annulus whose curved sides have length $2(1-\alpha)$ and $2(1+\alpha)$ (see Figure 2). Our bending boundary condition imposes such behavior:

$$\begin{cases} u(-1, y) = \dfrac{1-\alpha}{\alpha} \begin{pmatrix} \cos(\alpha y) \\ \sin(\alpha y) \end{pmatrix} & \text{for } y \in (-1, 1), \\ u(1, y) = \dfrac{1+\alpha}{\alpha} \begin{pmatrix} \cos(\alpha y) \\ \sin(\alpha y) \end{pmatrix} & \text{for } y \in (-1, 1). \end{cases} \tag{2.8}$$

This condition constrains only the left and right sides of the reference domain ($x = -1$ and $x = 1$).

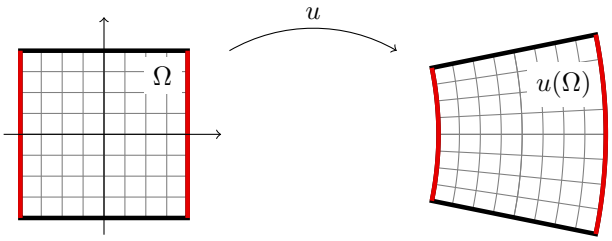

Fig. 2. The undeformed square, and its image. The image of the left and right boundaries is determined by our bending boundary condition (2.8). The grid shows the relaxed solution u^*, which is discussed in Section 2.3.

It makes perfect sense to consider the limit $\alpha \to 0$ (indeed, our scaling laws show how the energy depends on *both* α and ε as they approach 0). It may therefore

seem strange that our bending boundary condition (2.8) diverges as $\alpha \to 0$. But remember: the elastic and surface energy do not change if we subtract a constant from u. Subtracting the α-dependent constant $\alpha^{-1}(1,0)$ would assure that u fixes the points $(-1,0)$ and $(1,0)$ for all $\alpha > 0$, eliminating the apparent divergence. We do not include this translation in (2.8), since the formulas are simpler without it.

In summary: This paper studies the minimization of

$$E_\varepsilon[u] := \int_\Omega \operatorname{dist}^2(Du, K)\, dx\, dy + \varepsilon |D^2 u|(\Omega) \tag{2.9}$$

over $u \in W^{1,2}(\Omega;\mathbb{R}^2)$ such that $Du \in BV(\Omega;\mathbb{R}^{2\times 2})$, where u is constrained to satisfy the bending boundary condition (2.8) either approximately or exactly.

2.2. *The problem in physical variables*

We briefly discuss how our nondimensionalized problem (2.9) is related to the minimization of elastic plus surface energy in dimensional variables. To this end, let us consider a 2D strip of height $2H$ and width $2L$, and contemplate the minimization of

$$\int_{(-L,L)\times(-H,H)} \operatorname{dist}^2(Dv, K)\, d\tilde{x}\, d\tilde{y} + \delta |D^2 v|((-L,L)\times(-H,H)) \tag{2.10}$$

where $\delta > 0$ has the dimensions of length. The set K is the same as before – it is defined by (2.3) – since the deformation gradient is dimensionless. If $u(x,y) = L^{-1}v(Lx, Ly)$ then (2.10) is equal to

$$L^2 \left\{ \int_{(-1,1)\times(-H/L,H/L)} \operatorname{dist}^2(Du, K)\, dx\, dy + \frac{\delta}{L} |D^2 u|((-1,1)\times(-H/L,H/L)) \right\}, \tag{2.11}$$

which is the same as L^2 times our functional E_ε (with $\varepsilon = \delta/L$), except that the domain is $(-1,1)\times(-H/L,H/L)$ rather than $(-1,1)\times(-1,1)$.

While our mathematical results are presented, for simplicity, on a square domain, their extension to (a broad range of) rectangular domains is straightforward. Indeed, our upper bounds are in a certain sense periodic in y (see (3.4)), so they extend straightforwardly to rectangular domains provided that the height is larger than the vertical period. And while our lower bounds are stated for $\Omega = (-1,1)\times(-1,1)$, they extend straightforwardly to the domain $(-1,1)\times(-H/L,H/L)$ for any $H \geq L$, by recognizing that this rectangle contains $\lfloor H/L \rfloor$ disjoint copies of Ω and our bound applies to each one separately. (Actually, our lower bounds should also extend to the case where H/L is smaller than 1, provided H/L is large compared to the period of the relevant upper bound construction.)

2.3. *Solution of the relaxed problem*

It is natural to consider the case $\varepsilon = 0$ – in other words, the minimization of elastic energy alone. In view of Figure 1, we don't expect the minimum of the elastic energy

(subject to our bending boundary conditions) to be achieved. Rather, we expect a minimizing sequence to involve small-scale spatial oscillations, converging weakly to the solution of the associated relaxed variational problem. This subsection shows that the weak limit is unique, and identifies it.

The functional

$$E_0[u] = \int_\Omega \operatorname{dist}^2(Du, K)\, dx\, dy$$

is not lower semicontinuous. The theory of relaxation studies the asymptotic behavior of its minimizing sequences – characterizing, roughly speaking, the average behavior of low-energy states. More mathematically: the relaxed functional $E^*[u]$ is defined as the minimum of the possible limits of $E_0[u^j]$ along all sequences u^j converging to u in $L^1(\Omega;\mathbb{R}^2)$. In the present setting, where our integrand $W(F) = \operatorname{dist}^2(F, K)$ has quadratic growth at infinity, it can be shown to take the form[14,28]

$$E^*[u] = \int_\Omega W^{\mathrm{qc}}(Du)\, dx\, dy$$

where $W^{\mathrm{qc}} : \mathbb{R}^{2\times 2} \to \mathbb{R}$ is the quasiconvex envelope of the energy density W, defined by

$$W^{\mathrm{qc}}(F) := \inf_{\varphi \in W_0^{1,\infty}((0,1)^2;\mathbb{R}^2)} \int_{(0,1)^2} W(F + D\varphi)\, dx\, dy.$$

The set of minimizers of W^{qc}, in turn, is the *quasiconvex hull* of K, denoted by K^{qc}; it is the smallest quasiconvex set containing K. It is easy to see that $E^*[u] = 0$ if and only if $Du \in K^{\mathrm{qc}}$ almost everywhere; therefore once we have found K^{qc} it will be easy to identify the minimizer of the relaxed functional E^*. We therefore turn to the identification of K^{qc}.

Lemma 2.1. *For any $\alpha \in (0, \frac{1}{2}]$, the quasiconvex hull of the set K is given by*

$$K^{\mathrm{qc}} = \left\{ Q \begin{pmatrix} 1 & 0 \\ 0 & t \end{pmatrix} \ : \ Q \in \mathrm{SO}(2), \ \ t \in [1-\alpha, 1+\alpha] \right\}. \tag{2.12}$$

Proof. Let K^{qc} denote the quasiconvex hull of K. Then the Lemma asserts two inclusions: that K^{qc} is contained in the RHS of (2.12) and that K^{qc} contains the RHS of (2.12).

To prove the first inclusion, suppose $F \in K^{\mathrm{qc}}$. From the quasiconvexity of $\xi \mapsto \det \xi$ and of $\xi \mapsto -\det \xi$ we see that $\det F \in [1-\alpha, 1+\alpha]$, and by convexity of the norm we see that

$$|Fe_1| \le 1. \tag{2.13}$$

Using the identity

$$\det F = (Fe_1) \times (Fe_2)$$

and (2.13) we have

$$\det F \le |Fe_1|\,|Fe_2| \le |Fe_2|. \tag{2.14}$$

To conclude we consider the function $f(\xi) := |\xi e_2| - \det \xi$. Since $f(\xi) = 0$ for all $\xi \in K$, using the quasiconvexity of the determinant and hence of f, we have $f(\xi) \le 0$ for all $\xi \in K^{\rm qc}$, and in particular

$$|Fe_2| \le \det F. \tag{2.15}$$

Combining (2.14) and (2.15), we have

$$\det F = |Fe_2|.$$

It follows from (2.14) that $|Fe_1| = 1$ and $Fe_2 \perp Fe_1$. Hence F must have the form

$$F = a \otimes e_1 + ta^\perp \otimes e_2$$

for some $a \in S^1$, $t \in [1-\alpha, 1+\alpha]$. This shows that

$$K^{\rm qc} \subseteq \left\{ Q \begin{pmatrix} 1 & 0 \\ 0 & t \end{pmatrix} \;:\; Q \in {\rm SO}(2),\ t \in [1-\alpha, 1+\alpha] \right\}. \tag{2.16}$$

To prove the opposite inclusion, we fix a matrix F of the form

$$F = Q \begin{pmatrix} 1 & 0 \\ 0 & t \end{pmatrix}$$

for some $Q \in {\rm SO}(2)$ and $t \in [1-\alpha, 1+\alpha]$. If $t \in \{1 \pm \alpha\}$, then obviously $F \in K \subset K^{\rm qc}$. Assume now that $t \in (1-\alpha, 1+\alpha)$ and define

$$\tilde A := Q \begin{pmatrix} 1 & 0 \\ 0 & 1+\alpha \end{pmatrix} \text{ and } \tilde B := Q \begin{pmatrix} 1 & 0 \\ 0 & 1-\alpha \end{pmatrix}.$$

Then $\tilde A$, $\tilde B \in K$ and ${\rm rank}(\tilde A - \tilde B) = 1$, hence every convex combination of $\tilde A$ and $\tilde B$ belongs to $K^{\rm qc}$; in particular,

$$F = \frac{t-(1-\alpha)}{2\alpha}\tilde A + \frac{1+\alpha-t}{2\alpha}\tilde B \in K^{\rm qc}. \tag{2.17}$$

(The construction associated with (2.17) layers $\tilde A$ and $\tilde B$ in layers normal to $(0,1)$, with volume fractions given by their coefficients in (2.17). Thus, for any $F \in K^{\rm qc}$ we can infer the relative volume fractions of the two phases from (2.17).) Combining (2.16) and (2.17), the statement of Lemma follows. □

We next show that the relaxed problem with the boundary condition (2.8) has a unique minimizer.

Lemma 2.2. *Let $\alpha \in (0, \frac{1}{2}]$. Suppose that $u \in W^{1,\infty}(\Omega; \mathbb{R}^2)$ satisfies the boundary condition (2.8) and $Du \in K^{\rm qc}$ almost everywhere. Then $u \equiv u^*$ a.e., where*

$$u^*(x,y) := \frac{1+\alpha x}{\alpha} \begin{pmatrix} \cos(\alpha y) \\ \sin(\alpha y) \end{pmatrix}. \tag{2.18}$$

Proof. Using the boundary conditions in (2.8), we obtain that for almost every $y \in (-1,1)$ one has

$$\int_{-1}^{1} \partial_1 u(x,y)\,dx = u(1,y) - u(-1,y) = 2\begin{pmatrix}\cos(\alpha y)\\ \sin(\alpha y)\end{pmatrix},$$

which implies

$$2 = \left|\int_{-1}^{1} \partial_1 u\,dx\right| \le \int_{-1}^{1} |\partial_1 u|\,dx.$$

On the other hand, from $Du \in K^{\mathrm{qc}}$ almost everywhere, we have $|Du\,e_1| = |\partial_1 u| = 1$. Thus

$$2 = \left|\int_{-1}^{1} \partial_1 u\,dx\right|$$

is possible if and only if $\partial_1 u$ is constant in x (up to null sets). Using the boundary conditions (2.8) once again, we deduce that u must coincide with u^* given by (2.18). □

In view of the preceding Lemma, we call the function u^* given by (2.18) the *relaxed solution* of our variational problem. It takes the reference domain to an annulus, as shown in Figure 2. A brief calculation shows that

$$Du^*(x,y) = \begin{pmatrix}\cos(\alpha y) & -\sin(\alpha y)\\ \sin(\alpha y) & \cos(\alpha y)\end{pmatrix}\left[\frac{1+x}{2}\begin{pmatrix}1 & 0\\ 0 & 1+\alpha\end{pmatrix} + \frac{1-x}{2}\begin{pmatrix}1 & 0\\ 0 & 1-\alpha\end{pmatrix}\right], \quad (2.19)$$

so the relaxed solution represents our two phases layered (infinitesimally) with volume fractions $(1+x)/2$ and $(1-x)/2$, which (as expected) vary linearly in x.

The infimum of our elastic energy E_0 subject to the bending boundary condition is 0, since u^* achieves value 0 for the associated relaxed problem. However this infimum is not achieved:

Corollary 2.1. *Let $\alpha \in (0, \frac{1}{2}]$. If $u \in W^{1,2}(\Omega;\mathbb{R}^2)$ satisfies the boundary condition (2.8), then $E_0[u] > 0$. As a consequence, we also have $E_\varepsilon[u] > 0$ for any $\varepsilon > 0$.*

Proof. If $E_0[u]$ where 0, then Du would have to be in K almost everywhere. Since $K \subseteq K^{\mathrm{qc}}$, the previous Lemma applies and gives that $u = u^*$, whence $Du = Du^*$ almost everywhere. But one easily checks that $Du^* \notin K$ for $-1 < x < 1$ (for example because $|\partial_2 u^*| = |1 + \alpha x|$) – a contradiction. So $E_0[u] > 0$. Since the surface energy term is nonnegative, it follows immediately that $E_\varepsilon[u] > 0$. □

2.4. *Defining a microstructure with just one length scale*

In summarizing our results in the Introduction, we wrote in point (c) that one of our scaling laws applies to "constructions whose local length scale near the boundary is similar to that in the interior." To justify this statement in an ansatz-free setting, we need to make it more precise. Our approach is roughly as follows: we use the surface energy $|D^2 u|(\Omega)$ to estimate the typical length scale of u in the interior;

then we say u has a single length scale if, near the left and right boundaries, it doesn't mix the phases on a significantly smaller length scale. To make this precise, we start with what it means for u not to mix the two phases.

Definition 2.1. We say that $u \in W^{1,2}(\Omega;\mathbb{R}^2)$ *has no microstructure in* $\omega \subset \Omega$ *with constant* m for some $m \geq 1$, if

$$\min_{J\in\{A,B\}} \int_\omega \mathrm{dist}^2(Du, \mathrm{SO}(2)J)\, dx\, dy \leq m \int_\omega \mathrm{dist}^2(Du, K)\, dx\, dy. \tag{2.20}$$

While this definition depends on the choice of m, the choice is not very important; in practice, we shall often use $m = 2$. We view (2.20) as assuring that Du doesn't mix the two phases on a length scale smaller than the size of ω. To explain why, let $J = A$ be optimal for the left side of (2.20), and let ω_A and ω_B be the subsets of ω where Du is closest to $\mathrm{SO}(2)A$ and $\mathrm{SO}(2)B$ respectively. Then (2.20) assures that

$$c|\omega_B| \leq (m-1)\int_{\omega_A} \mathrm{dist}^2(Du, \mathrm{SO}(2)A)\, dx\, dy + m\int_{\omega_B} \mathrm{dist}^2(Du, \mathrm{SO}(2)B)\, dx\, dy$$

where c is a positive constant. If (as happens in our constructions) Du is everywhere close to one of the two wells – say, $\mathrm{dist}^2(Du, K) \leq \delta$ with δ small – then we can conclude that

$$(c - m\delta)|\omega_B| \leq (m-1)\delta|\omega|.$$

Since $m \geq 1$ this assures (if δ is small enough) that most of ω is in phase A.

We can now define our notion of a single-scale construction.

Definition 2.2. Let $m \geq 1$. Given any $u \in W^{1,2}(\Omega;\mathbb{R}^2)$, any $h \in (0,1]$, and any $y \in [-1, 1-h]$, we write $Q^h_\pm(y)$ for the squares at height y along the left and right boundaries,

$$Q^h_-(y) := (-1, -1+h) \times (y, y+h), \quad Q^h_+ := (1-h, 1) \times (y, y+h),$$

and we consider the sets of heights where u has no microstructure in these regions:

$$G^{m,h}_\pm := \{y \in (-1, 1-h) \,:\, u \text{ has no microstructure with constant } m \text{ in } Q^h_\pm(y)\}. \tag{2.21}$$

Using these notions, we define $S^{(m)}_{\text{onescale}}$ be the set of $u \in W^{1,2}(\Omega;\mathbb{R}^2)$ such that there is $h \in (0,1]$ which satisfies the following three conditions:

$$m\int_\Omega |D^2 u|\, dx\, dy \geq \frac{\alpha}{h}, \tag{2.22}$$

$$\mathcal{L}^1(G^{m,h}_+) \geq \frac{1}{m}, \tag{2.23}$$

$$\mathcal{L}^1(G^{m,h}_-) \geq \frac{1}{m}. \tag{2.24}$$

Informally: (2.22) assures that the typical length scale in the interior is at least of order h, while (2.23) and (2.24) assure the absence of microstructure on this length scale near the edges, for a significant fraction of heights y.

We shall show in Section 3 that a construction along the lines of Figure 1 is in $S^{(m)}_{\text{onescale}}$ for any $m \geq 2$. It is easy to see that a self-similar branching construction – in which the local length scale tends to zero near the left or right boundaries (as in the construction we use to prove Lemma 3.5) – does not belong to $S^{(m)}_{\text{onescale}}$ for any m.

Remark 2.1. It is clear from the definition that if $1 \leq m \leq m'$ then $G^{m,h}_{\pm} \subseteq G^{m',h}_{\pm}$ and therefore $S^{(m)}_{\text{onescale}} \subseteq S^{(m')}_{\text{onescale}}$.

2.5. *Statements of our main theorems*

Our theorems identify how the minimum energy scales with α and ε. The proofs carry additional information, of course: the proof of each upper bound identifies the scaling law of a particular test function; and the proof of each lower bound identifies an ansatz-free reason why no construction can achieve a better scaling law.

Our main results concern the energy (2.9) when our bending boundary condition (2.8) is imposed either exactly (Theorem 2.1) or else in a certain approximate sense (Theorem 2.2). When the boundary condition is imposed exactly the scaling law is $\alpha^{6/5}\varepsilon^{4/5}$, and it is achieved by a construction involving self-similar branching. When the boundary condition is imposed only up to an error of order $\alpha^{3/5}\varepsilon^{2/5}$ the energy scaling law remains the same, but it is also achieved by a single-scale construction along the lines of Figure 1.

It is natural to ask whether a single-scale construction can achieve the optimal scaling and also satisfy our bending boundary condition exactly. The answer is no: Theorem 2.3 shows that if we impose the boundary condition exactly and consider constructions with a single length scale then the energy scaling law changes to $\alpha^{5/4}\varepsilon^{3/4}$.

The attentive reader will have noticed the exponents of α and ε sum to 2 in both of the scaling laws just stated. We shall explain the reason for this in Remark 2.2.

We turn now to precise statements of our theorems, indicating for each how it follows from the upper bounds we prove in Section 3 and the lower bounds we prove in Section 4.

Theorem 2.1. *Let S_{ex} be the class of functions $u \in W^{1,2}(\Omega;\mathbb{R}^2)$ such that $u(\pm 1, y) = u^*(\pm 1, y)$ for almost all $y \in (-1,1)$. There is $c > 0$ such that for all $\alpha \in (0, 1/2]$ and all $\varepsilon \in (0, \alpha]$ we have*

$$\frac{1}{c}\alpha^{6/5}\varepsilon^{4/5} \leq \inf_{u \in S_{\text{ex}}} E_\varepsilon[u] \leq c\alpha^{6/5}\varepsilon^{4/5}.$$

Proof. The upper bound follows from Lemma 3.5, and the lower bound from Lemma 4.3. □

We remark that the same result holds if we assume $\varepsilon \in (0, M\alpha]$ for some $M \geq 1$, with a constant $c = c(M)$. Indeed, it suffices to apply the previous result to $E_{\varepsilon/M}$ and to use that $E_{\varepsilon/M} \leq E_\varepsilon \leq M E_{\varepsilon/M}$.

Theorem 2.2. *There are $c > 0$, $c_1 > 0$ with the following property. Let $S_{\rm app}$ be the set of all $u \in W^{1,2}(\Omega;\mathbb{R}^2)$ such that*

$$|u - u^*|(\pm 1, y) \le c_1 \alpha^{3/5} \varepsilon^{2/5} \text{ for all } y \in [-1,1]. \tag{2.25}$$

For all $\alpha \in (0, 1/2]$, all $\varepsilon \in (0, \alpha]$ and all $m \in [2, \infty)$ we have

$$\frac{1}{c}\alpha^{6/5}\varepsilon^{4/5} \le \inf_{u \in S_{\rm app}} E_\varepsilon[u] \le \inf_{u \in S_{\rm app} \cap S^{(m)}_{\rm onescale}} E_\varepsilon[u] \le c\alpha^{6/5}\varepsilon^{4/5}.$$

Proof. The lower bound follows from Lemma 4.3, where in particular the constant c_1 is introduced. The upper bound follows from Lemma 3.2, using that $S^{(2)}_{\rm onescale} \subseteq S^{(m)}_{\rm onescale}$ for $m \ge 2$. □

Theorem 2.3. *Let $S_{\rm ex}$ be as in Theorem 2.1, $m \ge 2$, and $S^{(m)}_{\rm onescale}$ as in Definition 2.2. There is $c_m > 0$ (depending only on m) such that for all $\alpha \in (0, 1/2]$, and all $\varepsilon \in (0, \alpha]$,*

$$\frac{1}{c_m}\alpha^{5/4}\varepsilon^{3/4} \le \inf_{u \in S_{\rm ex} \cap S^{(m)}_{\rm onescale}} E_\varepsilon[u] \le c_m \alpha^{5/4}\varepsilon^{3/4}.$$

Proof. The upper bound follows from Lemma 3.6, the lower bound from Lemma 4.4. □

Remark 2.2. As noted earlier, the exponents in our scaling laws sum to 2. To explain why this is natural, we observe that in the limit $\alpha \to 0$ one expects the elastic energy to be quadratic in α, while the surface energy is proportional to $\alpha\varepsilon$. Our upper-bound constructions do indeed have this property. For example, the energy of a construction like Figure 1 with microstructural length scale h turns out to be of order

$$\alpha^2 h^4 + \alpha\varepsilon h^{-1} = \alpha^2(h^4 + \frac{\varepsilon}{\alpha}h^{-1})$$

(see Lemma 3.1) and optimization in h gives $\alpha^2(\varepsilon/\alpha)^{4/5} = \alpha^{6/5}\varepsilon^{4/5}$. The emergence of the other scaling law is similar: when the construction motivated by Figure 1 is adjusted to near the boundary to achieve our exact bending boundary condition, the elastic energy changes to $\alpha^2 h^3$ (see (3.70)), so the preceding calculation changes to optimization of

$$\alpha^2 h^3 + \alpha\varepsilon h^{-1} = \alpha^2(h^3 + \frac{\varepsilon}{\alpha}h^{-1}),$$

which gives $\alpha^2(\varepsilon/\alpha)^{3/4} = \alpha^{5/4}\varepsilon^{3/4}$.

2.6. *Scientific context*

As we have already mentioned in the Introduction, this work is motivated by the modeling of martensitic phase transformation, where twinning with variable volume

fraction is seen in a number of different settings. The example that specifically motivates this paper involves the bending of a bar made from two martensite variants (a situation discussed theoretically in Ref. 31 and experimentally as well as theoretically in Refs. 3, 7). These papers discusses a situation slightly different from the thought-experiment represented by Figure 1: the unbent sample has pre-existing twins (which have no reason to be equally spaced). Bending makes the twin boundaries tilt, and also changes the spacing between them, establishing a highly-ordered periodic pattern similar to the deformed state shown in Figure 1. When the forces inducing bending are removed the twin boundaries return to their preferred orientations, while the spacing between them remains periodic. (As noted earlier, work subsequent to Ref. 7 on the same system revealed twinning on two distinct length scales,[8] a phenomenon also seen in similar experiments on other material systems.[9] Understanding this phenomenon using tools similar to those of the present paper remains a challenge for future work.)

This paper does not claim to model any of the systems just discussed. Indeed, as already noted in Section 2.1, our elastic energy is different from the one associated with a mixture of two martensite variants. Our goal is more methodological: to begin development of a mathematical toolkit for the analysis of twinning with variable volume fraction.

The bending of a bar is not the only setting where twinning with variable volume fraction seems to occur. Some other examples involving two martensite variants are discussed in Ref. 3 (see especially their Figure 4). Perhaps the "zigzag walls" seen in some ferroelastic and ferroeletric systems[15,26,27,30] can be viewed as examples. By the way, something similar has been seen in certain optimal design problems, since the optimal structures sometimes involve layered composites with varying volume fractions (see for example Section 1.3 of Ref. 18 and Figures 2 and 8 of Ref. 10).

Our work's mathematical context is the use of nonconvex variational problems to model the microstructures seen in materials that undergo martensitic phase transformations. Some of this work focuses on the elastic energy alone, without the inclusion of surface energy. Much attention has focused on determining, in various settings, where the quasiconvexification of the elastic energy is zero; this amounts to understanding which constant deformation gradients can be achieved by essentially stress-free microstructures. Without attempting a systematic review we note the seminal paper Ref. 2, which solved this problem for two compatible martensite variants in a 3D geometrically nonlinear setting. The book Ref. 4 discusses numerous examples using both geometrically linear and geometrically nonlinear models. Constructions involving twinning (and twins of twins, also known as laminates of order two or more) play a crucial role in this theory. In such constructions the volume fraction is constant (at least locally). The constructions in the present paper show (in the limit $\varepsilon \to 0$) that the class of essentially stress-free microstructures is not limited to those built from twinning with locally constant volume fraction.

The work discussed in the last paragraph ignored surface energy, whereas we include it. The point is that while the inclusion of surface energy produces a relatively

small change in the value of the energy, surface energy may nevertheless serve as a selection mechanism (preferring some constructions over others); moreover, within a given type of construction it should set the length scale of the microstructure. Actually, for the problems considered in this paper, it is not yet clear whether surface energy selects between the construction based on Figure 1 and the branched self-similar construction used to prove Lemma 3.5, since both achieve the same energy scaling law. However, within each of these constructions the presence of surface energy does, as expected, offer a prediction concerning local length scale of the microstructure.

There is a body of work exploring the influence of surface energy on constant-volume-fraction twinning in various settings. About 20 years ago Kohn and Müller suggested[21] that the essential physics of twinning near an austenite-twinned-martensite interface could be captured by the scalar variational problem

$$\min_{v_y=\pm 1} \int_\Omega v_x^2 \, dx \, dy + \varepsilon |v_{yy}|(\Omega) \tag{2.26}$$

in which v is a scalar-valued function defined on a rectangle $\Omega = (0, H) \times (0, L)$, with an additional term or boundary condition at $x = 0$ to model the effect of a neighboring region of austenite. Using this model, they obtained results in Ref. 23 concerning not only the energy scaling law but also the local length scale of the minimizer (see also Ref. 22 for an expository version). Subsequent work has improved our understanding of this scalar model and has obtained related results using fully-elastic models (see Refs. 5, 6, 12 for some recent developments and brief summaries of the literature).

It is natural to ask whether the methods developed in connection with constant-volume-fraction twinning can be adapted to the variable-volume-fraction setting. The present work addresses a particular instance of this question. Our arguments draw substantially on Refs. 5, 6 (and the self-similarly branched construction used to prove Lemma 3.5 has its roots in work on the scalar model problem (2.26)). We note, however, that the upper bound construction inspired by Figure 1 is basically new – though something analogous was considered in Ref. 25 for the scalar model (2.26) with boundary condition $v_y = 1$ at $x = 0$ and $v_y = -1$ at $x = L$.

Broadly speaking, the problem considered in this paper involves a nonconvex variational problem regularized by a higher-order term with a small coefficient. Problems of this type occur in many areas of physics. Understanding the defects and patterns that characterize the minimizers in a limit analogous to our $\varepsilon \to 0$ has sometimes been called the analysis of energy-driven pattern formation.[20] Without attempting to review the literature (which is by now vast), we note that these problems share some common features. Indeed, finding an upper bound on the minimum energy is conceptually straightforward, since it suffices to find a good test function (and nature often gives us a hint). Finding a good lower bound is usually more subtle, since the problem's nonconvexity means there is no tool analogous to convex duality. Successful treatments often start by showing that relaxed variational

problem (which characterizes the limits of minimizers as $\varepsilon \to 0$) has a unique solution; then one shows that $\varepsilon > 0$ forces deviation from the relaxed solution, and one estimates the energetic cost of that. This is indeed the conceptual basis of our lower bounds.

The results in this paper are limited to the energy scaling law; in other words, we prove upper and lower bounds that scale the same way in α and ε. The proofs never use any properties that would be specific to a minimizer (such as vanishing of the Euler-Lagrange equation or positivity of the second variation). Properties specific to a minimizer have been used in the setting of (2.26) in Refs. 11, 23 and are also at the heart of our forthcoming paper 24. In the setting of the present paper – where a construction inspired by Figure 1 and one using a self-similar branched construction share the same energy scaling law – we wonder whether arguments based on such properties might reveal whether the minimizer resembles one of these two very different constructions.

3. The upper bounds

3.1. *The upper bound in Theorem 2.2*

In this section we construct an appropriate test function in order to estimate the energy from above. Note that for $u = (u_1, u_2) \in W^{1,2}(\Omega; \mathbb{R}^2)$ we have

$$\operatorname{dist}^2(Du, K) = (\partial_x u_1 - \cos\theta)^2 + (\partial_x u_2 - \sin\theta)^2 + (\partial_y u_1 + \chi \sin\theta)^2 + (\partial_y u_2 - \chi\cos\theta)^2 \tag{3.1}$$

for some $\theta(x, y) \in [0, 2\pi)$ (rotation) and $\chi(x, y) \in \{1 - \alpha, 1 + \alpha\}$ (selection of the wells). Thus, the construction of a test function has the following ingredients:

[i] the test pattern $\tilde{\chi} = \tilde{\chi}_\varepsilon \in L^\infty(\Omega; \{1 - \alpha, 1 + \alpha\})$;
[ii] the test rotation $\tilde{\theta} = \tilde{\theta}_\varepsilon \in L^\infty(\Omega)$, and
[iii] the actual test function $\tilde{u} = \tilde{u}_\varepsilon \in W^{1,2}(\Omega; \mathbb{R}^2)$.

We decompose the strip $[-1, 1] \times \mathbb{R}$ in triangles as sketched in Figure 3. Specifically, we fix $h > 0$ and for $j \in \mathbb{Z}$ we set $y_j := jh$, and consider the triangles

$$T_j \text{ with vertices } ((-1)^{j+1}, y_j), ((-1)^j, y_{j-1}), ((-1)^j, y_{j+1}), \tag{3.2}$$

so that in particular the triangle T_0 has vertices in $(-1, 0)$, $(1, -h)$, and $(1, h)$, and the triangle T_1 has vertices in $(1, h)$, $(-1, 0)$, and $(-1, 2h)$.

The test pattern $\tilde{\chi}$ and the rotation $\tilde{\theta}$ are constant on each of the triangles, the test function $\tilde{u}$ is globally continuous and affine on each triangle. In suitable coordinates, the construction is periodic, in a sense made precise in (3.4) below. In order to avoid degeneracies in the case that the triangles are too large compared with Ω, we assume $h \le 1/4$. The main result is the following.

Lemma 3.1. *There is $c > 0$ such that the following holds. For any $\alpha \in (0, \frac{1}{2}]$ and $h \in (0, \frac{1}{4}]$ there is $u \in W^{1,2}_{\mathrm{loc}}((-1, 1) \times \mathbb{R}; \mathbb{R}^2)$ such that*

$$u(-1, 2jh) = u^*(-1, 2jh), \qquad u(1, (2j+1)h) = u^*(1, (2j+1)h) \ \text{ for all } j \in \mathbb{Z}, \tag{3.3}$$

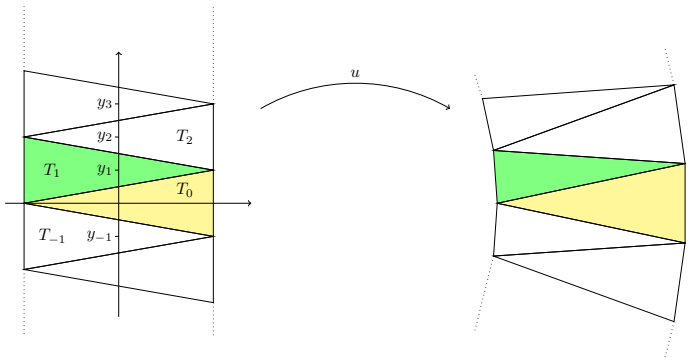

Fig. 3. Sketch of the piecewise affine construction of Lemma 3.1. We note that the set $u(\Omega)$ is different from $u^*(\Omega)$; in fact, the former is a polygonal approximation of the latter.

$$u(x, y + 2h) = Q_{2h\alpha} u(x, y) \qquad \text{where } Q_\theta := \begin{pmatrix} \cos\theta & -\sin\theta \\ \sin\theta & \cos\theta \end{pmatrix}, \tag{3.4}$$

which is continuous, piecewise affine, obeys the pointwise bounds

$$\operatorname{dist}(Du, K) \le c\alpha h^2, \tag{3.5}$$

$$|u - u^*|(\pm 1, y) \le \alpha h^2 \tag{3.6}$$

and

$$4\alpha \le |D^2 u|((-1, 1) \times (0, 2h]) \le c\alpha. \tag{3.7}$$

Further, $u_h\big|_\Omega \in S^{(2)}_{\text{onescale}}$.

Proof. We decompose $[-1, 1] \times \mathbb{R}$ in triangles according to (3.2). We set $u := u^*$ on all vertices of the triangles, and equal to the affine interpolation inside each triangle. This construction is automatically continuous and piecewise affine, and it obeys (3.3) by definition, and (3.4) because u^* does.

We prove (3.5). By (3.4) it suffices to do so in T_0 and T_1. We start with T_0. The definition of u gives

$$\begin{aligned} \partial_2 u|_{T_0} =& \frac{u^*(1, h) - u^*(1, -h)}{2h} = \frac{1 + \alpha}{2\alpha h} \left[\begin{pmatrix} \cos\alpha h \\ \sin\alpha h \end{pmatrix} - \begin{pmatrix} \cos\alpha h \\ -\sin\alpha h \end{pmatrix} \right] \\ =& (1 + \alpha) \frac{\sin\alpha h}{\alpha h} \begin{pmatrix} 0 \\ 1 \end{pmatrix} = \begin{pmatrix} 0 \\ 1 + \alpha + O(\alpha^2 h^2) \end{pmatrix} \end{aligned} \tag{3.8}$$

and

$$\begin{aligned} \partial_1 u|_{T_0} =& \frac{\frac{1}{2}(u^*(1, h) + u^*(1, -h)) - u^*(-1, 0)}{2} \\ =& \frac{1 + \alpha}{2\alpha} \begin{pmatrix} \cos\alpha h \\ 0 \end{pmatrix} - \frac{1 - \alpha}{2\alpha} \begin{pmatrix} 1 \\ 0 \end{pmatrix} = \begin{pmatrix} 1 + O(\alpha h^2) \\ 0 \end{pmatrix}. \end{aligned} \tag{3.9}$$

In particular, this implies

$$\operatorname{dist}(Du, K) \le |Du - A| \le c\alpha h^2 \text{ in } T_0. \tag{3.10}$$

To prove (3.6), we observe that $u(1, y) = u^*(1, y)$ for $y = \pm h$ and that $u(1, \cdot)$ is affine in $[-h, h]$. Also, we note that if g maps $[-h, h]$ to $\mathbb{R}^2$ with $g(-h) = g(h) = 0$ and $|\partial^2_{yy} g| \le \gamma$, then $|g(y)| \le \frac{1}{2}h^2\gamma$. (Indeed, for any unit vector $\xi \in \mathbb{R}^2$, $g \cdot \xi - \frac{\gamma}{2}(|y|^2 - h^2)$ is concave and $g \cdot \xi + \frac{\gamma}{2}(|y|^2 - h^2)$ is convex. Since each of these functions vanishes at $y = \pm h$, the first is nonnegative and the second is nonpositive.) Taking $g(y) = u(1, y) - u^*(1, y)$ gives $|u(1, y) - u^*(1, y)| \le \frac{1}{2}h^2 \sup |\partial^2_{yy} u^*| \le \frac{1}{2}(1+\alpha)\alpha h^2 \le \alpha h^2$. Therefore (3.6) holds in T_0.

We turn now to T_1. We have

$$u(-1, 0) = \frac{1-\alpha}{\alpha}\begin{pmatrix}1\\0\end{pmatrix}, \qquad u(1, h) = \frac{1+\alpha}{\alpha}\begin{pmatrix}\cos(\alpha h)\\ \sin(\alpha h)\end{pmatrix},$$

$$u(-1, 2h) = \frac{1-\alpha}{\alpha}\begin{pmatrix}\cos(2\alpha h)\\ \sin(2\alpha h)\end{pmatrix}.$$

Hence

$$\begin{aligned}\partial_2 u|_{T_1} = \frac{u(-1, 2h) - u(-1, 0)}{2h} =& (1-\alpha)\begin{pmatrix}(\cos(2\alpha h) - 1)/(2\alpha h)\\ \sin(2\alpha h)/(2\alpha h)\end{pmatrix}\\ =& (1-\alpha)\begin{pmatrix}-\alpha h + O(\alpha^3 h^3)\\ 1 + O(\alpha^2 h^2)\end{pmatrix}\end{aligned} \tag{3.11}$$

and

$$\partial_1 u|_{T_1} = \frac{1}{2}u(1, h) - \frac{1}{4}(u(-1, 0) + u(-1, 2h)) = \begin{pmatrix}1 + O(\alpha h^2)\\ \alpha h + O(\alpha^2 h^3)\end{pmatrix}. \tag{3.12}$$

Choosing the rotation $\tilde{\theta} := \alpha h$ in T_1, we conclude $\operatorname{dist}(Du, K) \le |Du - Q_{\alpha h} B| \le c\alpha h^2$ in T_1. Moreover, by arguments similar to those we used for T_0, we have $|u(-1, y) - u^*(-1, y)| \le \alpha h^2$ in T_1. This concludes the proof of (3.5) and (3.6).

We now turn to (3.7). From (3.8) and (3.11) we obtain

$$\partial_2 u_2|_{T_0} - \partial_2 u_2|_{T_1} = (1+\alpha)\frac{\sin(\alpha h)}{\alpha h} - (1-\alpha)\frac{\sin(2\alpha h)}{2\alpha h}$$

which gives

$$\begin{aligned}\left|\partial_2 u_2|_{T_0} - \partial_2 u_2|_{T_1} - 2\alpha\right| &= \left|(1+\alpha)(\frac{\sin(\alpha h)}{\alpha h} - 1) - (1-\alpha)(\frac{\sin(2\alpha h)}{2\alpha h} - 1)\right|\\ &\le 2\frac{1}{6}(2\alpha h)^2 \le \alpha\end{aligned}$$

where we used $0 < 1 - \frac{\sin t}{t} \le \frac{1}{6}t^2$ for $t \in (0, 1)$ and then $h \in (0, \frac{1}{4}]$. The same holds for $\partial_2 u_2|_{T_0} - \partial_2 u_2|_{T_{-1}}$. Therefore the jump of Du across the interfaces between triangles is larger than α; since the length of each interface is larger than 2 the first

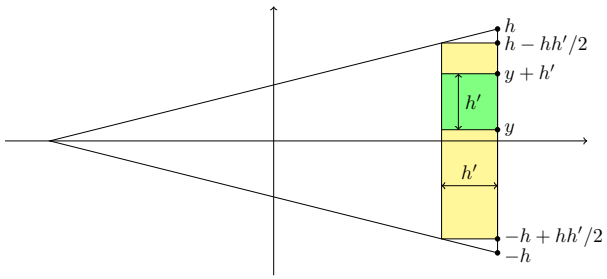

Fig. 4. Sketch of the proof that $u \in S^{(2)}_{\text{onescale}}$ in Lemma 3.1.

inequality in (3.7) follows. Using that there are at least $\frac{1}{h} - 2 \geq \frac{1}{2h}$ copies of the rectangle $(-1,1) \times (0,2h)$ inside Ω, we obtain

$$\int_{(-1,1)^2} |D^2 u| \, dx \, dy \geq (\frac{1}{h} - 2)4\alpha \geq \frac{2\alpha}{h}. \tag{3.13}$$

By the above computations we also easily obtain

$$|Du|_{T_0} - Du|_{T_1}| \leq c\alpha, \tag{3.14}$$

and with the periodicity this implies $|Du|_{T_2} - Du|_{T_1}| \leq c\alpha$. Condition (3.7) follows.

Finally, we prove that u has one scale in the sense of Definition 2.2. Let $h' := h/4$, $y \in H := (-h + hh'/2, h - h' - hh'/2)$. Then u is affine on the square $(1 - h', 1) \times (y, y + h') \subset T_0$ (see Figure 4), and in particular it has no microstructure in this set, so that $H \subset G^{2,h'}_+$. There are at least $2\lfloor \frac{1}{2h} \rfloor \geq \frac{1}{h} - 2 \geq \frac{1}{2h}$ disjoint copies of this set in $(-1,1)$, and $\mathcal{L}^1(H) = 2h - h' - hh' \geq \frac{3}{2}h$, hence $\mathcal{L}^1(G^{2,h'}_+) \geq \frac{1}{2}$. Similar arguments apply, of course, to $G^{2,h}_-$. Recalling (3.13) and the definition of h', this implies that $u \in S^{(2)}_{\text{onescale}}$. □

Lemma 3.2. *There is $c > 0$ such that for all $\alpha \in (0, 1/2]$ and all $\varepsilon \in (0, \alpha]$ there is $u \in S_{\text{app}} \cap S^{(2)}_{\text{onescale}}$ with*

$$E_\varepsilon[u_\varepsilon] \leq c\alpha^{6/5}\varepsilon^{4/5}. \tag{3.15}$$

Proof. The desired u will be provided by Lemma 3.1 with an appropriate choice of h. To be in S_{app}, u must satisfy

$$|u - u^*|(\pm 1, y)| \leq c_1\alpha^{3/5}\varepsilon^{2/5} \tag{3.16}$$

for all $y \in [-1,1]$ (see the statement of Theorem 2.2). For the present argument c_1 could be any positive constant; ultimately, its value must be taken to make the lower bound part of Theorem 2.2 true (so its value is set by Lemma 4.3). Our claim is that $h \leq 1/4$ can be chosen so that the u_h provided by Lemma 3.1 satisfies both (3.15) and (3.16). This is easy: since

$$|u_h - u^*|(\pm 1, y) \leq \alpha h^2 \quad \text{and} \quad E_\varepsilon[u_h] \leq c\alpha^2 h^4 + c\frac{\varepsilon\alpha}{h},$$

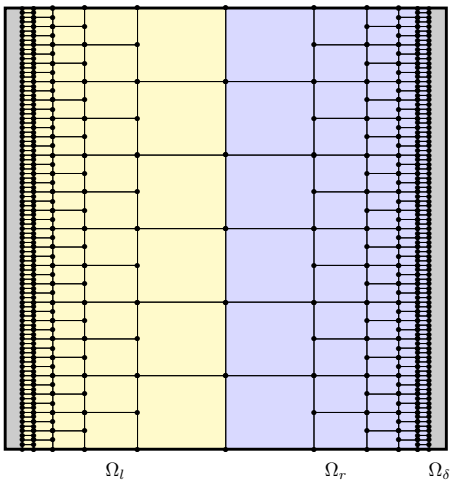

Fig. 5. Geometry of the construction in Section 3.2. The dots mark the points where u coincides with u^* and mark the periodicity (as usual, up to rotations); the gray areas are those where interpolation is used (called Ω_δ in the text). In each of the rectangles a period-doubling pattern as in Figure 7 is used.

it suffices to choose $h := \min\{\frac{1}{4}, c_1^{1/2}\}(\frac{\varepsilon}{\alpha})^{1/5}$. (This choice gives $h \leq 1/4$ because we assumed that $\varepsilon \leq \alpha$.) □

3.2. *The upper bound in Theorem 2.1*

This subsection constructs a test function that satisfies our bending boundary condition exactly. In this construction, the twins branch so that their length scale approaches zero near the boundary. Our treatment consists of three Lemmas. We start by constructing a piecewise affine discretization of the relaxed solution u^* in the vertical direction, described in Lemma 3.3. This discretization is used in Lemma 3.4 to introduce a period-doubling branching construction in a single box. Finally, Lemma 3.5 concludes the proof of the upper bound, by showing how to assemble the building blocks that were constructed in Lemma 3.4. The overall pattern of the period-doubling is shown in Figure 5.

Recall that the relaxed solution is

$$u^*(x,y) = (\frac{1}{\alpha} + x)f_y = \frac{1+\alpha x}{\alpha}\begin{pmatrix}\cos(\alpha y)\\ \sin(\alpha y)\end{pmatrix}, \quad f_y := \begin{pmatrix}\cos(\alpha y)\\ \sin(\alpha y)\end{pmatrix}. \tag{3.17}$$

In particular, $\partial_1 u^*(x,y) = f_y$ and $\partial_2 u^*(x,y) = (1+\alpha x) f_y^\perp$. As already observed in (2.19), at any $x \in [-1,1]$, the volume fraction of the phase $1 \pm \alpha$ is $\frac{1\pm x}{2}$.

We begin by introducing a discretization of u^* in the vertical direction on a segment $\{x_0\}\times[y_0-h, y_0+h]$, as illustrated in Figure 6. This is a continuous function which is affine on the three intervals which compose $[y_0-h, y_0+h] \setminus \{y_0 \pm h\frac{1-x_0}{2}\}$,

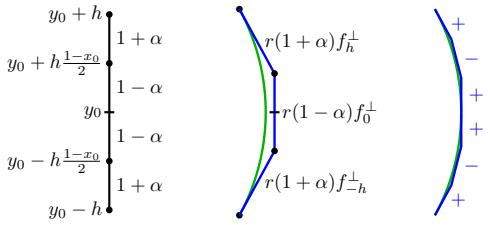

Fig. 6. Sketch of the discretization of u^*, see Lemma 3.3. Left: decomposition of the domain. Middle: $u^*(x_0,\cdot)$ (green arc) and its piecewise affine approximation v (blue). Right: same figure for two periods, as in the boundary conditions at x_b in Lemma 3.4.

coincides with u^* on the endpoints, and has (up to a factor) the same derivative as u^* at the endpoints and at the midpoint. Specifically, we have the following Lemma:

Lemma 3.3. *Let $\alpha \in (0, \frac{1}{2}]$, $h \in (0,1]$, $x_0 \in (-1,1)$, $y_0 \in \mathbb{R}$. Then there is a unique continuous map $v : [y_0-h, y_0+h] \to \mathbb{R}^2$ such that*

$$v(y_0+h) = u^*(x_0, y_0+h), \qquad v(y_0-h) = u^*(x_0, y_0-h), \tag{3.18}$$

and, for some $r > 0$,

$$v'(y) = r(1+\alpha) f^\perp_{y_0 \pm h} \text{ for } \pm(y-y_0) \in (h\frac{1-x_0}{2}, h) \tag{3.19}$$

and

$$v'(y) = r(1-\alpha) f^\perp_{y_0} \text{ for } |y-y_0| < h\frac{1-x_0}{2}. \tag{3.20}$$

Proof. The conditions on the derivative v' show that

$$\begin{aligned} v(y_0+h) - v(y_0-h) =& r(1-\alpha)h(1-x_0) f^\perp_{y_0} + r(1+\alpha)h\frac{1+x_0}{2}(f^\perp_{y_0+h} + f^\perp_{y_0-h}) \\ =& rh f^\perp_{y_0}[(1-\alpha)(1-x_0) + (1+\alpha)(1+x_0)\cos(\alpha h)] \\ =& rh f^\perp_{y_0}[2(1+\alpha x_0) + (1+\alpha)(1+x_0)(\cos(\alpha h)-1)]. \end{aligned}$$

From (3.17),

$$\begin{aligned} u^*(x_0, y_0+h) - u^*(x_0, y_0-h) =& \frac{1+\alpha x_0}{\alpha}(f_{y_0+h} - f_{y_0-h}) \\ =& \frac{1+\alpha x_0}{\alpha} 2\sin(\alpha h) f^\perp_{y_0}. \end{aligned}$$

We define $r_h : [-1,1] \to (0,\infty)$ by

$$r_h(x_0) := \frac{\sin(\alpha h)}{\alpha h}\left(1 - \frac{(1+\alpha)(1+x_0)}{2(1+\alpha x_0)}(1-\cos(\alpha h))\right)^{-1} \tag{3.21}$$

so that $v(y_0+h) - v(y_0-h) = u^*(x_0, y_0+h) - u^*(x_0, y_0-h)$. This concludes the definition of the discretization v on the segment $\{x_0\} \times [y_0-h, y_0+h]$. The argument just presented also proves uniqueness. □

Now we introduce the basic building block of our period-doubling construction.

Lemma 3.4. *There are $c, \lambda > 0$ with the following property. Let $-1 \le x_a < x_b \le 1$, $y_0 \in \mathbb{R}$, $h > 0$, $\ell := x_b - x_a$. Assume that $h \le \lambda \ell$ and $\alpha \in (0, \frac{1}{2}]$. Then there is $u : [x_a, x_b] \times \mathbb{R} \to \mathbb{R}^2$, $2h$-periodic in the second variable in the sense of (3.4), such that*

(i) $u(x, y_0 \pm h) = u^*(x, y_0 \pm h)$ for all $x \in [x_a, x_b]$,
(ii) $u(x_a, \cdot)$ is a discretization of u^* on $\{x_a\} \times [y_0 - h, y_0 + h]$ (the term "discretization" being understood in the sense of Lemma 3.3);
(iii) $u(x_b, y_0) = u^*(x_b, y_0)$, and $u(x_b, \cdot)$ is a discretization of u^* on both $\{x_b\} \times [y_0, y_0 + h]$ and $\{x_b\} \times [y_0 - h, y_0]$.

It also obeys

$$\operatorname{dist}(Du, K) \le c \frac{\alpha h^2}{\ell^2} \text{ pointwise}, \tag{3.22}$$

$$|Du - Du^*| \le c\alpha \text{ pointwise}, \tag{3.23}$$

and

$$|D^2 u|([x_a, x_b] \times [-1, 1]) \le c\alpha \frac{\ell}{h}. \tag{3.24}$$

The same holds if (ii) and (iii) are replaced by

(ii') $u(x_b, \cdot)$ is a discretization of u^* on $\{x_b\} \times [y_0 - h, y_0 + h]$;
(iii') $u(x_a, y_0) = u^*(x_a, y_0)$, and $u(x_a, \cdot)$ is a discretization of u^* on both $\{x_a\} \times [y_0, y_0 + h]$ and $\{x_a\} \times [y_0 - h, y_0]$.

The construction we present is parametrized by the shapes of the interfaces. In the proof, the interfaces will ultimately be determined by functions $g_0 \equiv 0$, $g_1(x)$, $g_2(x)$, $g_3(x)$ and $g_4 \equiv h$ (see Figure 7), though at the beginning of the argument we permit a larger or smaller number of interfaces, determined by an even integer N. Taking $N = 2$ and $g_0 \equiv 0$, $g_1(x) = h\frac{1-x}{2}$, $g_2 \equiv h$ in the construction used in the proof (with $x_a = -1$, $x_b = 1$) gives the piecewise affine construction from Lemma 3.1 (in particular, in this case the constant γ_1 defined by (3.33) takes the value $\gamma_1 = \alpha h$). However, this choice does not have the properties at x_b that are required by Lemma 3.4.

Proof. By periodicity, it suffices to construct u in the set $R := [x_a, x_b] \times [y_0 - h, y_0 + h]$. Without loss of generality we can assume $y_0 = 0$ and $\lambda \in (0, 1]$. We construct the function in $[x_a, x_b] \times [0, h]$ and then set

$$u(x, y) := \begin{pmatrix} u_1(x, -y) \\ -u_2(x, -y) \end{pmatrix} \text{ for } (x, y) \in [x_a, x_b] \times [-h, 0).$$

If $u_2(x, 0) = 0$ this does not introduce any discontinuity.

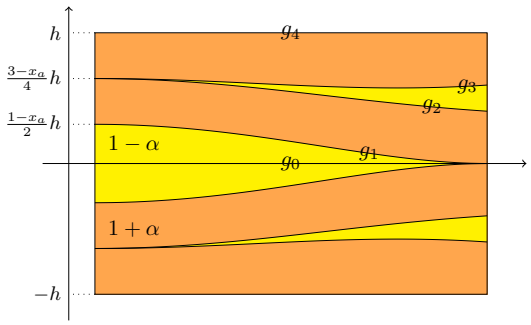

Fig. 7. Sketch of the construction in Lemma 3.4.

For N even (in the end we shall use $N = 4$), we consider functions $g_0, \dots, g_N : [x_a, x_b] \to [0, h]$ such that $0 = g_0 \le g_1 \le \cdots \le g_{N-1} \le g_N = h$ pointwise, see Figure 7. We assume that the regions (g_j, g_{j+1}) with j even are in the $1-\alpha$ phase, the ones with j odd are in the $1+\alpha$ phase. To keep notation simple we denote by $\alpha_j := (-1)^{j-1}\alpha$ the order parameter in the layer (g_j, g_{j+1}). The condition of having the appropriate volume fractions then becomes

$$\sum_{j=0}^{N-1} \alpha_j (g_{j+1} - g_j)(x) = \alpha x h, \tag{3.25}$$

which we assume to hold for all $x \in [x_a, x_b]$. This can be rewritten as $2\sum_{j=1}^{N-1} \alpha_j g_j = \alpha h(1-x)$. We shall choose the functions g_j so that

$$|g_j| \le h, \quad |g_j'| \le c\frac{h}{\ell}, \quad |g_j''| \le c\frac{h}{\ell^2}, \quad |g_j'''| \le c\frac{h}{\ell^3}. \tag{3.26}$$

We define $f_{(0)} := e_1$ and, for some function $\varphi \in C^2([x_a, x_b]; \mathbb{R})$ to be chosen below,

$$u(x, 0) := (\frac{1}{\alpha} + \varphi(x)) f_{(0)}.$$

This obeys $u_2(x, 0) = 0$, as required for the reflection to $[x_a, x_b] \times [-h, 0)$. Further, we require u to be continuous with

$$\partial_2 u(x, y) = \rho(x)(1 + \alpha_k) f_{(k)}^{\perp}(x) \qquad \text{if } g_k(x) < y < g_{k+1}(x), \tag{3.27}$$

where the functions $f_{(k)} \in C^2([x_a, x_b]; S^1)$ and $\rho \in C^2([x_a, x_b]; (0, \infty))$ are still to be chosen. This concludes the definition of u. Indeed, for $g_k(x) \le y \le g_{k+1}(x)$, one easily obtains

$$\begin{aligned} u(x, y) =& (\frac{1}{\alpha} + \varphi(x)) f_{(0)} + \rho(x) \sum_{j=0}^{k-1} (1 + \alpha_j) f_{(j)}^{\perp}(x)(g_{j+1} - g_j)(x) \\ &+ \rho(x)(1 + \alpha_k) f_{(k)}^{\perp}(y - g_k(x)). \end{aligned} \tag{3.28}$$

It remains to show that the various parameters can be chosen so that the stated properties are fulfilled.

We start from the nonlinear elastic energy. As the vertical derivative was already fixed in (3.27), we need to evaluate the horizontal one. In particular, the distance from K can be estimated by

$$\begin{aligned}\operatorname{dist}(Du,K) \leq & |Du-(f_{(k)}\otimes e_1+(1+\alpha_k)f_{(k)}^{\perp}\otimes e_2)|\\ \leq & |\partial_1 u - f_{(k)}| + |\partial_2 u - (1+\alpha_k)f_{(k)}^{\perp}|\\ \leq & |\partial_1 u - f_{(k)}| + 2|\rho-1|.\end{aligned} \tag{3.29}$$

The leading-order terms in $\partial_1 u$ will ultimately be those arising from the derivative of φ, which will be close to 1, and from the derivatives of the g_j functions. From (3.28) we obtain

$$\partial_1 u = f_{(0)} + \left[\sum_{j=0}^{k-1}(1+\alpha_j)(g'_{j+1}-g'_j) - (1+\alpha_k)g'_k\right] f_{(0)}^{\perp} + R \tag{3.30}$$

which implicitly defines a remainder term R, that will be estimated below. Since $g_0 = 0$, rearranging terms we obtain

$$\partial_1 u = f_{(0)} - \sum_{j=1}^{k} 2\alpha_j g'_j f_{(0)}^{\perp} + R. \tag{3.31}$$

Recalling (3.29), we define

$$f_{(k)} := \cos\gamma_k f_{(0)} + \sin\gamma_k f_{(0)}^{\perp} = \begin{pmatrix}\cos\gamma_k\\ \sin\gamma_k\end{pmatrix} \tag{3.32}$$

where

$$\gamma_k := -\sum_{j=1}^{k} 2\alpha_j g'_j. \tag{3.33}$$

From (3.26) we then obtain

$$|\gamma_k| \leq c\frac{\alpha h}{\ell}, \quad |\gamma'_k| \leq c\frac{\alpha h}{\ell^2}, \quad |\gamma''_k| \leq c\frac{\alpha h}{\ell^3}, \tag{3.34}$$

and correspondingly (recalling that $h \leq \ell$ to simplify the last estimate)

$$|f_{(k)} - f_{(0)}| \leq c\frac{\alpha h}{\ell}, \quad |f'_{(k)}| \leq c\frac{\alpha h}{\ell^2}, \quad |f''_{(k)}| \leq c\frac{\alpha h}{\ell^3}. \tag{3.35}$$

In particular, (3.31) gives

$$|\partial_1 u - f_{(k)}| \leq c|\gamma_k|^2 + |R| \leq c\frac{\alpha^2 h^2}{\ell^2} + |R|. \tag{3.36}$$

It remains to estimate the remainder term R. From (3.28) and (3.30) we obtain

$$\begin{aligned}|R| \leq |\varphi' - 1| &+ \sum_{j=0}^{k-1}(1+\alpha)|\rho f_{(j)} - f_{(0)}|\,|g'_{j+1} - g'_j| \\ &+ (1+\alpha)|\rho f_{(k)} - f_{(0)}|\,|g'_k| + |\rho'|(1+\alpha)h + \rho\sum_{j=0}^{k}(1+\alpha)|f'_{(j)}|h \qquad (3.37)\\ \leq |\varphi' - 1| &+ c\rho\frac{\alpha h^2}{\ell^2} + c|\rho - 1|\frac{h}{\ell} + 2|\rho'|h + c\rho\frac{\alpha h^2}{\ell^2}\end{aligned}$$

where in the second step we used (3.26) and (3.35) as well as $\alpha \leq \frac{1}{2}$. In particular, we conclude $|\partial_1 u - f_{(k)}| \leq c(\rho+1)\alpha h^2/\ell^2 + |\varphi' - 1| + c|\rho'|h + c|\rho - 1|h/\ell$.

Now we turn to the boundary conditions. This will lead to the choices of ρ and φ. From (3.28),

$$u(x,h) = (\frac{1}{\alpha} + \varphi(x))f_{(0)} + \rho(x)\sum_{j=0}^{N-1}(1+\alpha_j)f^{\perp}_{(j)}(x)(g_{j+1} - g_j)(x). \qquad (3.38)$$

We choose ρ so that the component along $f^{\perp}_{(0)}$ matches the boundary data. Indeed, by (3.32) we have $f^{\perp}_{(0)} \cdot f^{\perp}_{(j)} = f_{(0)} \cdot f_{(j)} = \cos\gamma_j$, and recalling (3.25) we obtain

$$\begin{aligned}f^{\perp}_{(0)} \cdot u(x,h) =&\rho(x)\sum_{j=0}^{N-1}(1+\alpha_j)(\cos\gamma_j(x))(g_{j+1} - g_j)(x)\\ =&\rho(x)\left[h(1+\alpha x) + \sum_{j=0}^{N-1}(1+\alpha_j)(\cos\gamma_j(x) - 1)(g_{j+1} - g_j)(x)\right].\end{aligned}$$

Since

$$f^{\perp}_{(0)} \cdot u^*(x,h) = \frac{1+\alpha x}{\alpha}\sin(\alpha h),$$

the mentioned boundary conditions is fulfilled if we choose

$$\rho(x) := \frac{\sin(\alpha h)}{\alpha h}\left[1 - \frac{1}{h(1+\alpha x)}\sum_{j=0}^{N-1}(1+\alpha_j)(1-\cos\gamma_j(x))(g_{j+1} - g_j)(x)\right]^{-1}.$$

We choose λ so that (3.34) implies $|\gamma_k| \leq \frac{\pi}{4}$. Then (recalling (3.25)) the value of the sum is in $[0, \frac{1}{2}h(1+\alpha x)]$, so that one does not divide by zero. Recalling (3.26) and (3.34), we estimate

$$|\rho - 1| \leq c\alpha^2\frac{h^2}{\ell^2}, \quad |\rho'| \leq c\alpha^2\frac{h^2}{\ell^3}, \quad |\rho''| \leq c\alpha^2\frac{h^2}{\ell^4}. \qquad (3.39)$$

This in particular implies $\rho \leq c$.

Now we use φ to fix the other component. From (3.38),

$$f_{(0)} \cdot u(x,h) = \frac{1}{\alpha} + \varphi(x) - \rho(x)\sum_{j=0}^{N-1}(1+\alpha_j)(\sin\gamma_j(x))(g_{j+1} - g_j)(x).$$

We require this to coincide with

$$f_{(0)} \cdot u^*(x,h) = \frac{1+\alpha x}{\alpha}\cos(\alpha h).$$

This defines φ,

$$\varphi(x) := \frac{(1+\alpha x)\cos(\alpha h)-1}{\alpha} + \rho(x)\sum_{j=0}^{N-1}(1+\alpha_j)(\sin\gamma_j(x))(g_{j+1}-g_j)(x),$$

which by (3.26), (3.34) and (3.39) obeys

$$|\varphi(x)-x| \le c\alpha\frac{h^2}{\ell}, \quad |\varphi'-1| \le c\alpha\frac{h^2}{\ell^2}, \quad |\varphi''| \le c\alpha\frac{h^2}{\ell^3}. \tag{3.40}$$

At this point $u = u^*$ on the top boundary; by symmetry the same holds on the bottom boundary. From (3.29), inserting (3.39), (3.36), (3.37), (3.40), and (3.39) again, we obtain the pointwise estimate

$$\operatorname{dist}(Du, K) \le c\alpha\frac{h^2}{\ell^2}. \tag{3.41}$$

The same computation, using $\alpha h \le 1$ and that (3.35) implies $|f_{(k)} - f_0| \le c\alpha$, leads to

$$|Du - \mathrm{Id}| \le |\partial_1 u - f_{(0)}| + |\partial_2 u - f_{(0)}^{\perp}| \le c\alpha$$

which, since the same holds for Du^*, proves (3.23).

It remains to choose the functions g_i, so that the conditions at the left and right boundary are fulfilled as well. We set $N = 4$ and observe that (3.25) is equivalent to

$$g_1(x) - g_2(x) + g_3(x) = \frac{1}{2}h(1-x), \tag{3.42}$$

which also gives $g_1' - g_2' + g_3' = -\frac{1}{2}h$. We require the functions g_i to match the required volume fractions and derivatives on the two sides, as in Figure 7. Specifically,

$$g_1(x_a) = h\frac{1-x_a}{2}, \qquad g_2(x_a) = g_3(x_a) = h\frac{3-x_a}{4}, \tag{3.43}$$

(the second value is arbitrarily fixed to be the average of $g_1(x_a)$ and $g_4(x_a) = h$) with

$$g_1'(x_a) = -\frac{1}{2}h, \qquad g_2'(x_a) = g_3'(x_a)$$

on the left, and

$$g_1(x_b) = 0, \quad g_2(x_b) = h\frac{1+x_b}{4}, \quad g_3(x_b) = h\frac{3-x_b}{4}, \tag{3.44}$$

with

$$g_1'(x_b) = 0, \quad g_2'(x_b) = \frac{1}{4}h, \quad g_3'(x_b) = -\frac{1}{4}h$$

on the right. It remains to interpolate these values to obtain functions which obey (3.42), $g_i \le g_{i+1}$, and (3.26). To do this we fix $\varphi \in C^\infty(\mathbb{R};[0,1])$ with $\varphi(t) = 1$ for $t \le$

0, $\varphi(t) = 0$ for $t \geq 1$, and set $g_i(x) := g_i^l(x)\varphi((x-x_a)/\ell) + g_i^r(x)(1-\varphi((x-x_a)/\ell))$, with $g_1^l(x) := h(1-x)/2$, $g_2^l(x) := g_3^l(x) := h(3-x)/4$, $g_1^r := 0$, $g_2^r(x) := h(1+x)/4$, $g_3^r(x) := h(3-x)/4$. The stated conditions follow.

We next verify the boundary conditions on the vertical sides. The definition (3.33) implies $\gamma_1 = -2\alpha g_1'$, $\gamma_2 = -2\alpha(g_1' - g_2')$, $\gamma_3 = -2\alpha(g_1' - g_2' + g_3')$ and

$$\gamma_1(x_a) = \gamma_3(x_a) = \alpha h, \quad \gamma_1(x_b) = 0, \quad \gamma_2(x_b) = \frac{1}{2}\alpha h, \quad \gamma_3(x_b) = \alpha h \tag{3.45}$$

(indeed, one can check that (3.25) leads in general to $\gamma_{N-1} = \alpha h$).

The function $y \mapsto u(x_a, y)$ is continuous, coincides with $u^*(x_a, y)$ for $y = h$ and $y = -h$, and by (3.27) obeys

$$\partial_2 u(x_a, y) = \rho(x_a)(1+\alpha) f_{(1)}^{\perp} \text{ for } g_1(x_a) < y < h,$$

$$\partial_2 u(x_a, y) = \rho(x_a)(1-\alpha) f_{(0)}^{\perp} \text{ for } |y| < g_1(x_a),$$

and, setting $f_{(-1)} := ((f_{(1)})_1, -(f_{(1)})_2)$,

$$\partial_2 u(x_a, y) = \rho(x_a)(1+\alpha) f_{(-1)}^{\perp} \text{ for } g_1(x_a) < -y < h.$$

Inserting the value of $\gamma_1(x_a)$ and $g_1(x_a)$ given above, we see that this satisfies the assumptions of Lemma 3.3. Therefore u obeys the boundary data on the left boundary. One can indeed check $\rho(x_a) = r_h(x_a)$, where r_h was defined in (3.21).

We now turn to the boundary on the right. For $y \in [0, h]$ we define $v(y) := u(x_b, y)$. By (3.27) and (3.44), this function obeys

$$v'(y) = \begin{cases} \rho(x_b)(1+\alpha) f_{(1)}^{\perp}(x_b), & \text{for } 0 < y < g_2(x_b), \\ \rho(x_b)(1-\alpha) f_{(2)}^{\perp}(x_b), & \text{for } g_2(x_b) < y < g_3(x_b), \\ \rho(x_b)(1+\alpha) f_{(3)}^{\perp}(x_b), & \text{for } g_3(x_b) < y < h. \end{cases}$$

By (3.45), $f_{(1)}(x_b) = f_0$, $f_{(2)}(x_b) = f_{h/2}$ and $f_{(3)}(x_b) = f_h$ (we use here the notation of (3.17)). Therefore

$$\frac{f_{h/2} \cdot v'(y)}{\rho(x_b)} = \begin{cases} (1+\alpha) f_{(1)}^{\perp}(x_b) \cdot f_{h/2} = (1+\alpha) \sin \frac{\alpha h}{2}, & \text{for } 0 < y < g_2(x_b), \\ (1-\alpha) f_{(2)}^{\perp}(x_b) \cdot f_{h/2} = 0, & \text{for } g_2(x_b) < y < g_3(x_b) \\ (1+\alpha) f_{(3)}^{\perp}(x_b) \cdot f_{h/2} = -(1+\alpha) \sin \frac{\alpha h}{2}, & \text{for } g_3(x_b) < y < h. \end{cases}$$

By (3.44) the first and the last segment have the same length, therefore

$$f_{h/2} \cdot v(0) = f_{h/2} \cdot v(h).$$

By (3.17), the same holds for $u^*(x_b, \cdot)$. Since we already checked that $v(h) = u^*(x_b, h)$, we obtain $f_{h/2} \cdot v(0) = f_{h/2} \cdot u^*(x_b, 0)$. By construction $v_2(0) = 0$, which corresponds to $f_0^{\perp} \cdot v(0) = f_0^{\perp} \cdot u^*(x_b, 0)$. As the two vectors are linearly independent, we conclude that $v(0) = u^*(x_b, 0)$. Therefore v satisfies the assumptions of Lemma 3.3 with $y_0 = h/2$, and u obeys the stated boundary data.

Finally, we estimate the surface energy. The interfaces have length bounded by $c\ell$, and by (3.23) the jump across the interface (including the boundary of the box)

is bounded by $c\alpha$. Further, by (3.27) $\partial_2\partial_2 u = 0$, $|\partial_1\partial_2 u| \leq \alpha h/\ell^2$, and from (3.28) one obtains $|\partial_1\partial_1 u| \leq c\alpha h/\ell^2$ (the leading-order term is the one arising from g_j''). We conclude that

$$|D^2 u|((x_a, x_b) \times (-h, h)) \leq c\alpha\ell + c\alpha\frac{h^2}{\ell}. \tag{3.46}$$

Hence,

$$|D^2 u|((x_a, x_b) \times [-1, 1]) \leq c\alpha\frac{\ell}{h} + c\alpha\frac{h}{\ell} \leq c\alpha\frac{\ell}{h},$$

where in the final step we used $h \leq \ell$ once again. The second assertion follows from the same argument, swapping x_a and x_b in the definition of the functions g_i in (3.43) and the following equations. □

We are now ready to state and prove the main result in this subsection.

Lemma 3.5. *There is $C > 0$ such that for any $\alpha \in (0, \frac{1}{2}]$ and $\varepsilon \in (0, \alpha]$ there exists $u_\varepsilon \in S_{\rm ex}$ (the class defined in Theorem 2.1), such that*

$$E_\varepsilon[u_\varepsilon] < C\alpha^{6/5}\varepsilon^{4/5}.$$

Proof. Since the proof is long, we present it in a sequence of steps. The general structure of the construction is illustrated in Figure 5.

Step 1: Outline. We shall treat separately the part on the left and the part on the right, and for this preliminary discussion let us focus on the set on the right, $\Omega_r := [0, 1] \times [-1, 1]$. One difficulty, which is common to many branching constructions for problems where the singular perturbation fully controls a higher-order derivative (here, the Hessian of u), is that branching of the microstructure cannot go down to scale zero, but has instead to stop a certain point, which we denote here with $\{x = 1 - \delta\}$ for some $\delta \in (0, 1)$ chosen below (indeed, branching down to scale 0 would contradict the trace theorem). This condition corresponds to the assumption $h \leq \lambda\ell$ in Lemma 3.4. The length scale of the microstructure in $u(1 - \delta, \cdot)$ will also be δ (see (3.49)–(3.51) below for details). We then introduce a boundary layer in which the test function w will be the interpolation between the boundary condition u^* and the branching construction u. In Steps 2 and 3 we present the branching construction in the central part $[-1 + \delta, 1 - \delta] \times [-1, 1]$ and estimate its energy using Lemma 3.4. Step 4 provides the energy estimate for the interpolant in the boundary layer Ω_δ, thus concluding the construction of the test function.

Step 2: Test function away from the boundary. In $[-1 + \delta, 1 - \delta] \times [-1, 1]$ we shall implement the technique of global domain branching.

At $x = 0$ assume that we have oscillations of period $h_0 \in (0, 1]$ (the value of h_0 will be chosen below). The function u we intend to construct will be such that $u(0, \cdot)$ is a discretization of $u^*(0, \cdot)$ on scale h_0, in the sense of Lemma 3.3. We remark that

the discretization treats the $1+\alpha$ and the $1-\alpha$ phase slightly differently, therefore the final construction is not going to be symmetric on the two sides. This can be solved using the first assertion in Lemma 3.4 for the "refining" on the right-hand side, and the second one for the "coarsening" on the left-hand side.

Precisely, we fix $\mu := \frac{1}{2^{1+b}}$, for some $b > 0$ to be chosen later, and let

$$l_i := c_0 \mu^{i+1}, \quad h_i := \frac{h_0}{2^i}, \ i \geq 0,$$

where $c_0 = c_0(b)$ is chosen such that $\sum_{i=0}^{\infty} l_i = 1$. For any $k \in \mathbb{N}$ and $j \in \mathbb{Z}$ we also define

$$x_k := \sum_{i=0}^{k-1} l_i, \text{ and } y_{k,j} := j h_k.$$

We are now in position to apply the first assertion in Lemma 3.4 in every box $[x_k, x_{k+1}] \times [y_{k,j}, y_{k,j+1}]$, which has size $l_k \times h_k$ (provided that $h_k \leq \lambda l_k$), and thus to define the test function

$$u(x,y) := u_{k,j}(x,y), \qquad (x,y) \in [x_k, x_{k+1}] \times [y_{k,j}, y_{k,j+1}]$$

for $k = 1, ..., I$ and $j = -2^{k-1} n_0, ..., 2^{k-1} n_0 - 1$. At the same time we use the second assertion in Lemma 3.4 in every box $[-x_{k+1}, -x_k] \times [y_{k,j}, y_{k,j+1}]$, which also has size $l_k \times h_k$; one easily checks that the resulting function is continuous on all interfaces.

Note that, by construction, for fixed k, Du has $2^k n_0$ oscillations in the vertical direction with period h_k. At each branching step k the number of such boxes doubles. Furthermore, since $b \neq 0$, at every step the ratio of l_k to h_k changes, and the branching process continues as long as $h_k \leq \lambda l_k$, where $\lambda \in (0,1]$ is the constant from Lemma 3.4. This condition implicitly defines the number of branching steps I.

Step 3: Energy estimate away from the boundary. At this point, for fixed $I \geq 2$ (to be chosen later), let us estimate the energy of I steps of the branching construction,

$$E[u, [0, x_{I+1}] \times [-1,1]] \leq \sum_{i=0}^{I} \left[\int_{x_i}^{x_{i+1}} \int_{-1}^{1} \operatorname{dist}^2(Du, K)\, dy\, dx + \varepsilon |D^2 u|([x_i, x_{i+1}] \times [-1,1]) \right]$$
$$\leq C \sum_{i=0}^{I} \left[l_i \frac{\alpha^2 h_i^4}{l_i^4} + \varepsilon \frac{\alpha l_i}{h_i} \right] \leq C \sum_{i=0}^{I} \left[\alpha^2 h_0^4 \frac{1}{(16\mu^3)^i} + \varepsilon \frac{\alpha}{h_0} (2\mu)^i \right]. \quad (3.47)$$

Choosing μ such that $16\mu^3 > 1$ and $2\mu < 1$, which means

$$0 < b < \frac{1}{3}, \quad (3.48)$$

each term in the sum belongs to a converging geometric series, and, since the estimates on the other side are identical,

$$E_I := E[u, [-x_{I+1}, x_{I+1}] \times [-1, 1]] \leq C\left(\alpha^2 h_0^4 + \frac{\varepsilon\alpha}{h_0}\right).$$

The value of b will be fixed for the rest of the proof, for example one can take $b = 1/6$. At this point we set $h_0 := \min\{1, \frac{1}{4}\lambda c_0\mu\}\left(\frac{\varepsilon}{\alpha}\right)^{1/5}$. This way

$$E_I \leq c\alpha^2 h_0^4 + c\frac{\alpha\varepsilon}{h_0} \leq C\alpha^{6/5}\varepsilon^{4/5}.$$

We define

$$I := \text{ the largest integer such that } h_I \leq \lambda l_I \tag{3.49}$$

which implies that

$$h_I \leq \lambda l_I \quad \text{and} \quad \lambda\mu l_I = \lambda l_{I+1} < h_{I+1} = \frac{1}{2}h_I, \quad \text{hence } l_I \sim h_I \text{ and } (2\mu)^I \sim h_0. \tag{3.50}$$

We remark that $h_0 \leq \frac{1}{4}c_0\mu$ ensures $I \geq 2$.

Step 4: Boundary layer near the $x = 1$ boundary. Fix

$$\delta := 1 - x_{I+1} = c'\mu^I, \tag{3.51}$$

where c' depends only on μ, and recall that $\Omega_\delta := [1 - 2\delta, 1] \times [-1, 1]$. Let $\varphi_\delta \in C^\infty([0, 1]; [0, 1])$ with $\varphi_\delta \equiv 1$ for $x < 1 - 2\delta$ and $\varphi_\delta \equiv 0$ for $x > 1 - \delta = x_{I+1}$, $|\varphi_\delta'| \leq 2/\delta$, $|\varphi_\delta''| \leq c/\delta^2$. Define the interpolation function as

$$w := u\varphi_\delta + u^*(1 - \varphi_\delta).$$

This way

$$Dw = (Du - Du^*)\varphi_\delta + (u - u^*) \otimes D\varphi_\delta + Du^*.$$

First, note that (3.50) and (3.51) imply $l_I \sim h_I \sim \delta$. By construction, $u(1 - \delta, y) - u^*(1 - \delta, y)$ is h_I-periodic (in the sense of (3.4)), with $u(1 - \delta, 0) - u^*(1 - \delta, 0) = 0$. With (3.23),

$$|u - u^*| \leq c\alpha\delta^2 \qquad \text{in } \Omega_\delta.$$

Since w is an interpolant between u and u^*, uniformly in Ω_δ we have

$$|w - u^*| \leq c\alpha\delta \tag{3.52}$$

and

$$|Dw - Du^*| \leq c\alpha, \tag{3.53}$$

Finally, we observe that

$$\operatorname{dist}(Du^*, K) \leq c\alpha \text{ in } \Omega. \tag{3.54}$$

Combining the estimates (3.52), (3.53) and (3.54), we get the following estimate for the elastic energy in the boundary layer:

$$\int_{\Omega_\delta} \mathrm{dist}^2(Dw, K)\, dx\, dy \le C\alpha^2\delta.$$

Using (3.51), $\mu = 2^{-1-b}$, (3.50), $h_0 \sim (\varepsilon/\alpha)^{1/5}$ and (3.48), we have

$$\alpha^2\delta \sim \alpha^2\mu^I \sim \alpha^2\left[\left(\frac{1}{2}\right)^I\right]^{1+b} \sim \alpha^2 h_0^{\frac{1+b}{b}} \sim \alpha^2\left(\frac{\varepsilon}{\alpha}\right)^{\frac{1+b}{5b}} \le \alpha^2\left(\frac{\varepsilon}{\alpha}\right)^{4/5}.$$

It remains to estimate the surface energy near the boundary. Note that

$$D^2w = (u-u^*)\otimes D^2\varphi + 2(Du-Du^*)\otimes D\varphi_\delta + \varphi_\delta D^2u + (1-\varphi_\delta)D^2u^*.$$

Using (3.52), we have

$$\varepsilon\int_{(1-2\delta,1-\delta)\times(-1,1)} |D^2\varphi|\,|u-u^*|\,dx\,dy \le c\varepsilon\delta\frac{1}{\delta^2}\alpha\delta \le c\alpha\varepsilon.$$

Similarly, by (3.23), we have

$$\varepsilon\int_{(1-2\delta,1-\delta)\times(-1,1)} |Du-Du^*|\,|D\varphi_\delta|\,dx\,dy \le c\varepsilon\delta\alpha\frac{1}{\delta} \le c\alpha\varepsilon.$$

Next, using (3.24), with $h \sim l \sim \delta$ and the explicit form of u^*, we have

$$\varepsilon|D^2u|((1-2\delta,1-\delta)\times(-1,1)) \le c\varepsilon\alpha \text{ and } \varepsilon\int_{\Omega_\delta}|D^2u^*|\,dx\,dy \le c\varepsilon\delta\alpha.$$

Altogether, recalling $\delta \le 1$ and $\varepsilon \le \alpha$,

$$\varepsilon|D^2w|(\Omega_\delta) \le c\alpha\varepsilon \le c\alpha^{6/5}\varepsilon^{4/5}.$$

The same holds on $\hat\Omega_\delta := [-1,-1+2\delta]\times[-1,1]$, using $\hat\varphi_\delta(x) := \varphi_\delta(-x) \in C^\infty([-1,0];[0,1])$ instead of φ_δ, which leads to the same estimates.

To summarize, for all $\varepsilon \in (0,\alpha]$ we have constructed a continuous function u which satisfies $u \equiv u^*$ at $x = 1$ and $x = -1$, and such that

$$E_\varepsilon[u;\Omega] \le C\alpha^{6/5}\varepsilon^{4/5}. \tag{3.55}$$

3.3. *The upper bound in Theorem 2.3*

Lemma 3.6. *There exists $C > 0$ such that for any $\alpha \in (0, \frac{1}{2}]$ and $\varepsilon \in (0,\alpha]$ there is $u_\varepsilon \in S_{\mathrm{ex}} \cap S^{(2)}_{\mathrm{onescale}}$, as defined in Theorem 2.3, such that we have*

$$E_\varepsilon[u_\varepsilon] < C\alpha^{5/4}\varepsilon^{3/4}.$$

Proof. The main idea is to modify the test function $\tilde u$, described in the proof of Lemma 3.1, in order to meet the required boundary conditions. We fix $h \in (0, \frac{1}{6}]$, chosen below. The geometry $\tilde\chi$ and the rotation $\tilde\theta$ will be unchanged, and the periodicity condition (3.3) still holds. Recall that the triangle T_0 has vertices

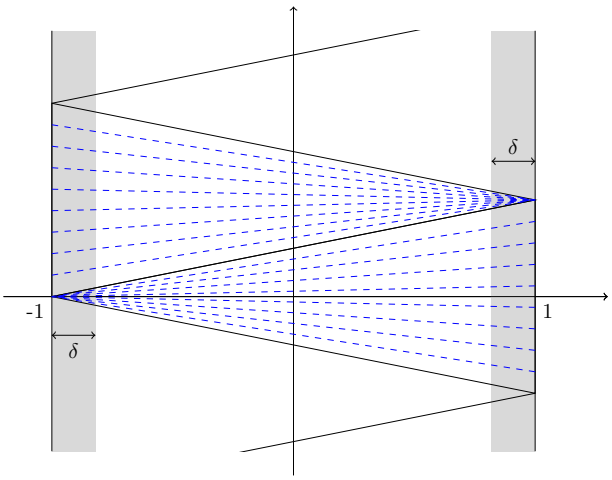

Fig. 8. Sketch of the construction used in the proof of Lemma 3.6. The two triangles T_0 and T_1 are shown, the blue dashed lines are the directions of interpolation in the definition of w_h. The gray area is R_δ.

in $(-1,0)$, $(1,h)$, and $(1,-h)$, and the triangle T_1 has vertices in $(-1,0)$, $(1,h)$, and $(-1,2h)$. Due to the periodic nature of this test configuration, it suffices to construct the test function in T_0 and T_1 only. We refer to Figure 8 for a sketch and start with the construction in T_0:

(i) Let u_h be the piecewise affine function, constructed in Lemma 3.1. By (3.10), in T_0 this function satisfies $|Du_h - A| \leq c\alpha h^2$.

(ii) Next we define the nonlinear interpolated construction w_h. Set $w_h = u^*$ for $x = -1$ and $x = 1$, and in each triangle define the affine interpolation between the tip and the base. Precisely, in T_0, which is the set where $|y| \leq h(1+x)/2$, we use the boundary values

$$u^*(-1,0) = \frac{1-\alpha}{\alpha} e_1 \quad \text{and} \quad u^*(1,y) = \frac{1+\alpha}{\alpha} \begin{pmatrix} \cos(\alpha y) \\ \sin(\alpha y) \end{pmatrix}.$$

Define (in T_0)

$$\begin{aligned} w_h(x,y) :=& \frac{1-x}{2} u^*(-1,0) + \frac{1+x}{2} u^*(1, y\frac{2}{1+x}) \\ =& \frac{1-x}{2}\frac{1-\alpha}{\alpha} e_1 + \frac{1+x}{2}\frac{1+\alpha}{\alpha} \begin{pmatrix} \cos(2\alpha y/(x+1)) \\ \sin(2\alpha y/(x+1)) \end{pmatrix}. \end{aligned}$$

We compute

$$\partial_2 w_h = (1+\alpha) \begin{pmatrix} -\sin(2\alpha y/(x+1)) \\ \cos(2\alpha y/(x+1)) \end{pmatrix} \tag{3.56}$$

and

$$\partial_1 w_h = -\frac{1-\alpha}{2\alpha}e_1 + \frac{1+\alpha}{2\alpha}\begin{pmatrix}\cos(2\alpha y/(x+1))\\ \sin(2\alpha y/(x+1))\end{pmatrix} - \frac{y(1+\alpha)}{x+1}\begin{pmatrix}-\sin(2\alpha y/(x+1))\\ \cos(2\alpha y/(x+1))\end{pmatrix}. \tag{3.57}$$

Since $|y| \le h(x+1)$, we have

$$\begin{aligned}\partial_1 w_h &= -\frac{1-\alpha}{2\alpha}e_1 + \frac{1+\alpha}{2\alpha}(e_1 + \frac{2\alpha y}{x+1}e_2 + O(\alpha^2 h^2)) - (1+\alpha)\frac{y}{x+1}(e_2 + O(\alpha h))\\ &= e_1 + O(\alpha h)\end{aligned}$$

and

$$\partial_2 w_h = (1+\alpha)e_2 + O(\alpha h).$$

Therefore

$$|Dw_h - A| + |Dw_h - Du_h| \le c\alpha h \text{ pointwise in } T_0. \tag{3.58}$$

(iii) Fix $\delta \in (0, 1/2]$ (we shall take $\delta = h$ at the end), and let $\varphi_\delta \in C_c^\infty((-1,1);[0,1])$ with $\varphi_\delta = 1$ on $(-1+\delta, 1-\delta)$, $|\varphi_\delta'| \le 2/\delta$ and $|\varphi_\delta''| \le c/\delta^2$. We define

$$v(x,y) := \varphi_\delta(x)u_h(x,y) + (1-\varphi_\delta(x))w_h(x,y).$$

Clearly, this function is continuous and obeys the boundary condition (2.8). We compute

$$Dv = \varphi_\delta Du_h + (1-\varphi_\delta)Dw_h + \varphi_\delta'(u_h - w_h)\otimes e_1. \tag{3.59}$$

Introduce

$$R_\delta := [1-\delta, 1]\times[-1,1] \cup [-1, -1+\delta]\times[-1,1].$$

We first observe that $v = u_h$ in $T_0 \setminus R_\delta$ and therefore by (i)

$$\operatorname{dist}(Dv, K) \le |Dv - A| \le c\alpha h^2 \text{ pointwise in } T_0 \setminus R_\delta. \tag{3.60}$$

It remains to estimate the elastic energy in R_δ. From (3.58) and the fact that $w_h = u_h = u^*$ on the vertices of T_0 we obtain

$$|w_h - u_h| \le c\alpha h(h+\delta) \text{ pointwise in } T_0 \cap R_\delta. \tag{3.61}$$

Therefore

$$\begin{aligned}|Dv - A| \le& \varphi_\delta|Du_h - A| + (1-\varphi_\delta)|Dw_h - A| + |\varphi_\delta'|\,|w_h - u_h|\\ \le& c\alpha h + c\frac{\alpha h^2}{\delta}.\end{aligned} \tag{3.62}$$

At this point we set $\delta = h$ and obtain

$$\int_{T_0\cap R_\delta} \operatorname{dist}^2(Dv, K)\,dx\,dy \le c\alpha^2 h^4. \tag{3.63}$$

Having completed the construction of our test function v in T_0, we turn now to the region T_1. Since the construction of v in T_1 is analogous to what we did in T_0, we shall be relatively brief:

(i) Recall that in T_1 the test function u_h in Lemma 3.1 satisfies $|Du_h - Q_{\alpha h}B| \leq c\alpha h^2$.

(ii) Since T_1 is the set where $|y-h| \leq h(1-x)/2$, we have the following boundary values:

$$u^*(1,h) = \frac{1+\alpha}{\alpha}\begin{pmatrix}\cos(\alpha h)\\ \sin(\alpha h)\end{pmatrix} \quad \text{and} \quad u^*(-1,y) = \frac{1-\alpha}{\alpha}\begin{pmatrix}\cos(\alpha y)\\ \sin(\alpha y)\end{pmatrix} \quad \text{for } y \in [0,2h].$$

Define (in T_1)

$$\begin{aligned} w_h(x,y) :=& \frac{1+x}{2}u^*(1,h) + \frac{1-x}{2}u^*\left(-1, \frac{-2y+h(x+1)}{x-1}\right) \\ =& \frac{1+x}{2}\frac{1+\alpha}{\alpha}\begin{pmatrix}\cos(\alpha h)\\ \sin(\alpha h)\end{pmatrix} + \frac{1-x}{2}\frac{1-\alpha}{\alpha}\begin{pmatrix}\cos\left(\alpha\frac{-2y+h(x+1)}{x-1}\right)\\ \sin\left(\alpha\frac{-2y+h(x+1)}{x-1}\right)\end{pmatrix}. \end{aligned}$$

The inequality

$$|y-h| \leq \frac{(1-x)h}{2} \text{ in } T_1$$

implies

$$\left|\frac{-2y+h(x+1)}{x-1}\right| = \left|h + \frac{2}{1-x}(y-h)\right| \leq 2h. \tag{3.64}$$

Using (3.64), direct computation yields

$$\partial_1 w_h = e_1 + O(\alpha h)$$

and

$$\partial_2 w_h = (1-\alpha)e_2 + O(\alpha h).$$

Comparing with the corresponding value of the gradient of u_h, we conclude that

$$|Dw_h - Q_{\alpha h}B| + |Dw_h - Du_h| \leq c\alpha h \text{ pointwise in } T_1. \tag{3.65}$$

The remaining energy estimate in T_1 is exactly the same as in T_0, hence (using the same interpolation φ_δ)

$$\int_{T_1 \cap R_\delta} \operatorname{dist}^2(Dv, K)\, dy\, dx \leq c\alpha^2 h^4 \tag{3.66}$$

for $\delta = h$.

Having completed the construction in T_0 and T_1, we extend it using periodicity to all of Ω (just as we did in the proof of Lemma 3.1). We verify that w_h coincides

with u^* on the top and bottom boundaries of the triangles, and in particular that it is continuous. Using (3.63), (3.66) and (3.60), we have

$$\int_\Omega \mathrm{dist}^2(Dv,K)\,dy\,dx \le \frac{1}{h}\int_{(T_0\cup T_1)\cap R_\delta} \mathrm{dist}^2(Dv,K)\,dy\,dx + \frac{1}{h}\int_{(T_0\cup T_1)\setminus R_\delta} \mathrm{dist}^2(Dv,K)\,dy\,dx \le \frac{1}{h}\left(C_1\alpha^2h^4 + C_2\alpha^2h^4\right) \le C\alpha^2h^3. \quad (3.67)$$

We now estimate the surface energy $\int_\Omega |D^2v|\,dx\,dy$. In $\Omega\setminus R_\delta$ we have $v\equiv u_h$ and we may proceed as in Lemma 3.1. In $T_0\cap R_\delta$, we have

$$D^2v = (u_h-w_h)D^2\varphi_\delta + 2(Du_h-Dw_h)D\varphi_\delta + \varphi_\delta D^2u_h + (1-\varphi_\delta)D^2w_h. \quad (3.68)$$

Since $|D\varphi_\delta|\le\frac{C}{\delta}$ and $|D^2\varphi_\delta|\le\frac{C}{\delta^2}$, using (3.58) and (3.61), for $\delta=h$ the first two terms in (3.68) are estimated as

$$|(u_h-w_h)D^2\varphi_\delta + 2(Du_h-Dw_h)D\varphi_\delta| \le \frac{C}{\delta^2}\alpha h(h+\delta) + \frac{C}{\delta}\alpha h \le C\alpha.$$

Next, differentiating the explicit expressions for Dw_h given by (3.57) and (3.56), it is straightforward to see that for some $C>0$ we have $|D^2w_h|(x,y)\le C\alpha/(1+x)$ for all $(x,y)\in T_0\cap R_\delta$, and by explicit integration $|D^2w_h|(T_0\cap R_\delta)\le C\alpha\delta h$. Finally, $D^2u_h=0$ in T_0 since it is an affine function. Altogether, we have

$$|D^2v|(T_0\cap R_\delta)\le C\alpha\delta h.$$

Using analogous reasoning, we have

$$|D^2v|(T_1\cap R_\delta)\le C\alpha\delta h$$

as well. Let us now estimate the jump of Dv across the interface between $T_0\cap R_\delta$ and $T_1\cap R_\delta$. Using (3.59), as well as (3.61), (3.58) and (3.65), we have

$$|Dv-Du_h|\le c_0\alpha h \text{ both in } T_0\cap R_\delta \text{ and in } T_1\cap R_\delta.$$

Hence, using (3.14), we have

$$|Dv|_{T_0} - Dv|_{T_1}| \le |Du_h|_{T_0} - Du_h|_{T_1}| + 2c_0\alpha h \le c_1\alpha.$$

The above estimates, summed over $\sim\frac{1}{h}$ triangles using periodicity, yield

$$\int_{\Omega\cap R_\delta} |D^2v|\,dx\,dy \le C\alpha,$$

and therefore, using Lemma 3.1 once again,

$$\varepsilon\int_\Omega |D^2v|\,dx\,dy \le \frac{C\varepsilon\alpha}{h}. \quad (3.69)$$

Combining the elastic energy contribution (3.67) and the surface energy contribution (3.69), we have

$$E_\varepsilon[v] \le C\left(\alpha^2h^3 + \frac{\alpha\varepsilon}{h}\right). \quad (3.70)$$

Before choosing the value of h, we verify that v has one scale in the sense of Definition 2.2. Since $v \equiv u_h$ in $\Omega \setminus R_h$, which covers a fraction $1-h$ of the interfaces, by Lemma 3.1 (see (3.13)) we have

$$\int_\Omega |D^2 v|\, dx\, dy \geq \int_{\Omega\setminus R_h} |D^2 u_h|\, dx\, dy \geq \left(\frac{1}{h} - 2\right)(1-h)4\alpha = \frac{4\alpha}{h}(1-2h)(1-h) \geq \frac{2\alpha}{h},$$

provided that $h \leq \frac{1}{6}$.

Next, arguing as in the proof of Lemma 3.1, we define $h' := h/4$ and $y \in H := (-h + hh'/2, h - h' - hh'/2)$ and a square $S' := (1-h', 1) \times (y, y+h') \subset T_0$. We shall now use the fact that for any $\xi \in \mathbb{R}^{2\times 2}$:

$$\mathrm{dist}(\xi, \mathrm{SO}(2)A) < \alpha \Longrightarrow \mathrm{dist}(\xi, K) = \mathrm{dist}(\xi, \mathrm{SO}(2)A).$$

Indeed, since $\mathrm{dist}(\mathrm{SO}(2)A, \mathrm{SO}(2)B) = |A - B| = 2\alpha$, we have

$$\mathrm{dist}(\xi, \mathrm{SO}(2)B) \geq \mathrm{dist}(\mathrm{SO}(2)A, \mathrm{SO}(2)B) - \mathrm{dist}(\xi, \mathrm{SO}(2)A) > \alpha.$$

In our case, using (3.62) in $S' \subset T_0$ there is $c_2 > 0$ such that

$$\mathrm{dist}(Dv, \mathrm{SO}(2)A) \leq |Dv - A| \leq c_2 \alpha h.$$

If $c_2 h \leq 1$ then this is smaller than α, and therefore

$$\int_{S'} \mathrm{dist}^2(Dv, \mathrm{SO}(2)A)\, dx\, dy = \int_{S'} \mathrm{dist}^2(Dv, K)\, dx\, dy.$$

This implies that v has no microstructure in S', so that $H \subset G_+^{2,h'}$. The rest of the proof is identical to the arguments in Lemma 3.1, and yields $v \in S^{(2)}_{\mathrm{onescale}}$.

Finally, we set $h := \min\{\frac{1}{6}, c_2^{-1}\}\frac{\varepsilon^{1/4}}{\alpha^{1/4}}$. This choice satisfies all the conditions imposed above, and using (3.70) it gives the desired upper bound

$$E_\varepsilon[v] \leq C\alpha^{5/4}\varepsilon^{3/4}. \qquad \square$$

4. The lower bounds

4.1. *The lower bound parts of Theorems 2.1 and 2.2*

We start with a simplified version of the proof, which shows the origin of the $\varepsilon^{4/5}$ scaling without resolving how the prefactor depends on α in the limit $\alpha \to 0$.

Lemma 4.1. *For any $\alpha \in (0, \frac{1}{2}]$ there is $C_\alpha > 0$ such that for any $\varepsilon \in (0, \alpha]$, and any $u \in W^{1,2}(\Omega; \mathbb{R}^2)$ satisfying the boundary conditions*

$$u(\pm 1, y) = u^*(\pm 1, y) \tag{4.1}$$

one has

$$E_\varepsilon[u] \geq C_\alpha \varepsilon^{4/5}.$$

Proof. The strategy is similar to the one of Ref. 5. Let $u \in W^{1,2}(\Omega; \mathbb{R}^2)$ which obeys (4.1) and let $E := E_\varepsilon[u]$. If $E \geq 1$ the proof is concluded, hence we can assume $E < 1$ in the following.

Fix $\ell \in (0, \frac{1}{2}]$, to be chosen later. We choose a strip $S := (-1, 1) \times (y_0, y_0 + \ell) \subset \Omega$ (see Figure 9) such that

$$\int_S [\mathrm{dist}^2(Du, K) + \varepsilon |D^2 u|] \, dx \, dy \leq \ell E, \tag{4.2}$$

where as usual $\int_S |D^2 u| dx dy$ is interpreted as $|D^2 u|(S)$ if u is not in $W^{2,1}(S; \mathbb{R}^2)$.

Within this strip we choose a square $Q := (x_0, x_0 + \ell) \times (y_0, y_0 + \ell)$ such that $x_0 \in (-\frac{1}{2}, \frac{1}{2})$ and

$$\int_Q [\mathrm{dist}^2(Du, K) + \varepsilon |D^2 u|] \, dx \, dy \leq \ell^2 E. \tag{4.3}$$

By the BV version of Poincaré's inequality there is an $\hat{F} \in \mathbb{R}^{2\times 2}$ with

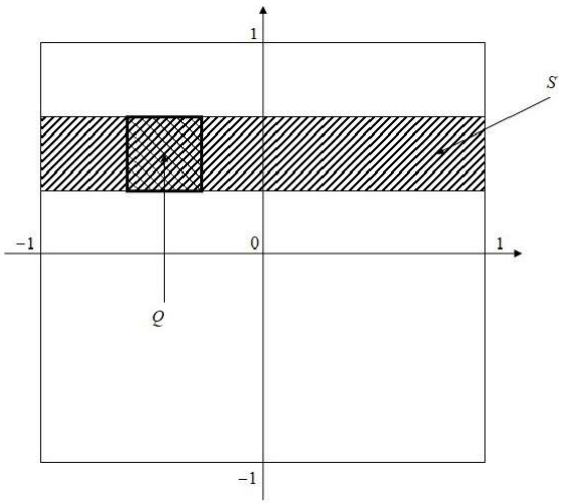

Fig. 9. Choice of the strip S and the square Q in the proofs of Lemmas 4.1 and 4.3.

$$\|Du - \hat{F}\|_{L^1(Q)} \leq c\ell |D^2 u|(Q) \leq c\ell^3 E/\varepsilon. \tag{4.4}$$

Let F_* be the matrix in K that's closest to $\hat{F}$. Then

$$|\hat{F} - F_*| \leq |\hat{F} - Du(x)| + \mathrm{dist}(Du(x), K).$$

This inequality is true since F_* is chosen such that the line segment from $\hat{F}$ to F_* is the shortest path from $\hat{F}$ to K, so it is shorter than the path that goes from $\hat{F}$ to $Du(x)$ then to the point of K closest to that. Integrating the latter inequality over Q, together with (4.3) and (4.4), we have

$$\|Du - F_*\|_{L^1(Q)} \leq \|Du - \hat{F}\|_{L^1(Q)} + \|\hat{F} - F_*\|_{L^1(Q)} \leq c\ell^3 \varepsilon^{-1} E + c\ell^2 E^{1/2}.$$

Using Poincaré's inequality once again, there is $b \in \mathbb{R}^2$ such that

$$\left\| u - F_* \begin{pmatrix} x \\ y \end{pmatrix} - b \right\|_{L^1(Q)} \leq C \left(\frac{\ell^4 E}{\varepsilon} + \ell^3 E^{1/2} \right). \tag{4.5}$$

For $y \in (y_0, y_0 + \ell)$ we set

$$f_y := \begin{pmatrix} \cos(\alpha y) \\ \sin(\alpha y) \end{pmatrix} \qquad \text{and} \qquad e(y) := \int_{(-1,1)} \operatorname{dist}^2(Du, K)\, dx.$$

By $\partial_1 u^* = f_y$, the fundamental theorem of calculus and (4.1), for almost all such y we have

$$\int_{-1}^{1} (f_y - \partial_1 u(x,y))\, dx = (u^* - u)(1,y) - (u^* - u)(-1,y) = 0. \tag{4.6}$$

Let $\theta \in L^\infty((-1,1))$ and $\sigma \in L^\infty((-1,1); \{1-\alpha, 1+\alpha\})$ be such that

$$\operatorname{dist}(Du(x,y), K) = |Du - Q_\theta F_\sigma| \qquad \text{for almost all } x \in (-1,1), \tag{4.7}$$

where as usual $Q_\theta := \begin{pmatrix} \cos\theta & -\sin\theta \\ \sin\theta & \cos\theta \end{pmatrix}$ and $F_\sigma := e_1 \otimes e_1 + \sigma e_2 \otimes e_2$. We set $e_\theta := Q_\theta e_1$, so that (4.7) and Hölder's inequality imply

$$\int_{-1}^{1} |\partial_1 u - e_\theta|\, dx \leq \int_{-1}^{1} |Du - Q_\theta F_\sigma|\, dx = \int_{-1}^{1} \operatorname{dist}(Du, K)\, dx \leq \sqrt{2} e^{1/2}(y). \tag{4.8}$$

We write, using (4.6),

$$\begin{aligned} \int_{-1}^{1} f_y \cdot (f_y - e_\theta)\, dx &= \int_{-1}^{1} f_y \cdot (f_y - \partial_1 u(x,y))\, dx + \int_{-1}^{1} f_y \cdot (\partial_1 u(x,y) - e_\theta)\, dx \\ &\leq \int_{-1}^{1} f_y \cdot (f_y - \partial_1 u(x,y))\, dx + \int_{-1}^{1} \operatorname{dist}(Du(x,y), K)\, dx \\ &\leq \sqrt{2} e^{1/2}(y). \end{aligned}$$

Since $|f_y| = |e_\theta| = 1$, we have $|f_y - e_\theta|^2 = 2 f_y \cdot (f_y - e_\theta)$. Therefore

$$\int_{-1}^{1} |f_y - e_\theta|^2\, dx = 2 \int_{-1}^{1} f_y \cdot (f_y - e_\theta)\, dx \leq 2\sqrt{2} e^{1/2}(y).$$

Finally, with a triangular inequality and using again (4.8) and Hölder's inequality,

$$\begin{aligned} \int_{-1}^{1} |\partial_1 u - \partial_1 u^*|\, dx &\leq \int_{-1}^{1} |\partial_1 u - e_\theta|\, dx + \int_{-1}^{1} |e_\theta - f_y|\, dx \\ &\leq \sqrt{2} e^{1/2}(y) + 2\sqrt{2} e^{1/4}(y). \end{aligned}$$

This implies

$$|u(x,y) - u^*(x,y)| \leq c e^{1/2}(y) + c e^{1/4}(y).$$

Integrating over Q and using (4.2), this leads to

$$\begin{aligned}\int_Q |u(x,y)-u^*(x,y)|\,dx\,dy \le& c\ell\int_{y_0}^{y_0+\ell}[e^{1/2}(y)+e^{1/4}(y)]\,dy\\ \le& c\ell(\ell E^{1/2}+\ell E^{1/4}) \le c\ell^2E^{1/4}\end{aligned} \tag{4.9}$$

since $E\le 1$. Recalling (4.5) and using the triangle inequality we obtain that there is $F_*\in K$ such that

$$\int_Q \left|F_*\begin{pmatrix}x\\y\end{pmatrix}-b-f_y\frac{1+\alpha x}{\alpha}\right|dx\,dy \le C[\ell^2E^{1/4}+\frac{\ell^4E}{\varepsilon}+\ell^3E^{1/2}].$$

With Lemma 4.2 below, we get

$$c\alpha\ell^3 \le \ell^2E^{1/4}+\frac{\ell^4E}{\varepsilon}+\ell^3E^{1/2},$$

or

$$E\ge c_\alpha\min\{\ell^4,\frac{\varepsilon}{\ell},1\}=c_\alpha\min\{\ell^4,\frac{\varepsilon}{\ell}\}.$$

Setting $\ell:=\frac14\varepsilon^{1/5}$ yields the desired lower bound

$$E\ge c_\alpha\varepsilon^{4/5}. \qquad \square$$

Lemma 4.2. *There is $c>0$ such that for any $F\in K$, $\ell\in(0,\frac14]$, $x_0\in[-\frac12,\frac12]$, $y_0\in\mathbb{R}$, $b\in\mathbb{R}^2$, $\alpha\in(0,1]$, we have*

$$\int_{(x_0,x_0+\ell)\times(y_0,y_0+\ell)}\left|F\begin{pmatrix}x\\y\end{pmatrix}-b-f_y\frac{1+\alpha x}{\alpha}\right|dx\,dy\ge c\alpha\ell^3. \tag{4.10}$$

Proof. Let $q:=(x_0,x_0+\ell)\times(y_0,y_0+\ell)$, and define $v:q\to\mathbb{R}^2$ by

$$v(x,y)=F\begin{pmatrix}x\\y\end{pmatrix}-b-f_y\frac{1+\alpha x}{\alpha}.$$

We compute

$$Dv(x,y)=F-f_y\otimes e_1-(1+\alpha x)f_y^\perp\otimes e_2,$$

and observe that, since $|Fe_2|=1+s\alpha$ for some $s\in\{\pm1\}$ and $|f_y|=1$,

$$|Dv|\ge|Fe_2-(1+\alpha x)f_y^\perp|\ge|(1+s\alpha)-(1+\alpha x)|=\alpha|s-x|\ge\frac14\alpha,$$

since $x\in(x_0,x_0+\ell)\subset[-\frac12,\frac34]$. In particular, $\|Dv\|_{L^1(q)}\ge\frac14\alpha\ell^2$. Further,

$$\partial_xDv(x,y)=-\alpha f_y^\perp\otimes e_2\quad\text{and}\quad\partial_yDv(x,y)=-\alpha f_y^\perp\otimes e_1+\alpha(1+\alpha x)f_y\otimes e_2$$

imply $|D^2v|\le4\alpha$ pointwise, and therefore $\|D^2v\|_{L^1(q)}\le4\alpha\ell^2$. By the Gagliardo interpolation inequality

$$\|Dv\|_{L^1(q)}\le c\|v\|_{L^1(q)}^{1/2}\|D^2v\|_{L^1(q)}^{1/2}+c\ell^{-1}\|v\|_{L^1(q)},$$

which holds for any square q of side ℓ with a universal constant, we deduce

$$\|v\|_{L^1(q)} \geq c \min\left\{ \ell \|Dv\|_{L^1(q)}, \frac{\|Dv\|^2_{L^1(q)}}{\|D^2 v\|_{L^1(q)}} \right\} \geq c \min\{\alpha\ell^3, \alpha\ell^2\} = c\alpha\ell^3,$$

which is the assertion. □

We now give the general proof of the lower bound.

Lemma 4.3. *There are $c_1 > 0$ and $C > 0$ such that for any $\alpha \in (0, \frac{1}{2}]$, any $\varepsilon \in (0, \alpha]$, and any $u \in W^{1,2}(\Omega; \mathbb{R}^2)$ satisfying the boundary conditions*

$$|u - u^*|(\pm 1, y) \leq \delta \tag{4.11}$$

for some $\delta \leq c_1 \alpha^{3/5} \varepsilon^{2/5}$ one has

$$E_\varepsilon[u] \geq C \alpha^{6/5} \varepsilon^{4/5}.$$

The proof starts as the simplified one above. We present a self-contained proof, replicating a couple of initial steps; in particular, the choice of S and Q is identical.

Proof. Let $u \in W^{1,2}(\Omega; \mathbb{R}^2)$ with $|u - u^*|(\pm 1, y) \leq \delta$, and let $E := E_\varepsilon[u]$. If $E \geq 1$ (this includes in particular the case that $D^2 u$ is not a bounded measure) there is nothing to prove, so we can assume $E < 1$ in the following.

Step 1. We choose a good strip and a good section.
Fix $\ell \in (0, \frac{1}{16}]$, to be chosen later. We choose a strip $S := (-1, 1) \times (y_0, y_0 + \ell) \subset \Omega$ (see Figure 9) such that

$$\int_S [\mathrm{dist}^2(Du, K) + \varepsilon |D^2 u|] \, dx \, dy \leq \ell E, \tag{4.12}$$

and within this strip a square $Q := (x_0, x_0 + \ell) \times (y_0, y_0 + \ell)$ such that $(x_0, x_0 + \ell) \subseteq (-\frac{3}{4}, \frac{3}{4})$ and

$$\int_Q [\mathrm{dist}^2(Du, K) + \varepsilon |D^2 u|] \, dx \, dy \leq \ell^2 E. \tag{4.13}$$

By Poincaré's inequality there is an $\hat{F} \in \mathbb{R}^{2\times 2}$ with $\|Du - \hat{F}\|_{L^1(Q)} \leq c\ell |D^2 u|(Q) \leq c\ell^3 E/\varepsilon$, and by the first term in (4.13) there is $F_* \in K$ with $\|Du - F_*\|_{L^1(Q)} \leq c\ell^3 \varepsilon^{-1} E + c\ell^2 E^{1/2}$. We choose $x_* \in (x_0, x_0 + \ell)$ such that

$$\int_I |Du(x_*, y) - F_*| dy \leq c\ell^2 \varepsilon^{-1} E + c\ell E^{1/2}, \tag{4.14}$$

where $I := (y_0, y_0 + \ell)$.

Step 2. We use (4.12) *to obtain control on $\partial_1(u - u^*)$.*
We recall that

$$\partial_1 u^*(x, y) = f_y := \begin{pmatrix} \cos(\alpha y) \\ \sin(\alpha y) \end{pmatrix}.$$

By the fundamental theorem of calculus, for almost all $y \in I$ we have

$$\int_{-1}^{1} (\partial_1 u(x,y) - f_y)\, dx = (u-u^*)(1,y) - (u-u^*)(-1,y).$$

At this point the proof differs from the previous one. To obtain the appropriate scaling in α it is important to separate the longitudinal component of Du, on which we have better control, from the tangential one.

We take the component along f_y and recall the boundary condition (4.11) to obtain

$$-2\delta \le \int_{-1}^{1} f_y \cdot (\partial_1 u(x,y) - f_y)\, dx \le 2\delta. \tag{4.15}$$

We observe that, by the structure of K,

$$|\partial_1 u| \le \min_{a\in S^1} (|a| + |\partial_1 u - a|) \le 1 + \operatorname{dist}(Du, K). \tag{4.16}$$

For a fixed $y \in I$ we define $g : (-1,1) \to \mathbb{R}$ by $g(x) := f_y \cdot \partial_1 u(x,y) - 1$, and then set $g_+ := \max\{0, g\}$, $g_- := \max\{0, -g\}$. From (4.15) we obtain

$$-2\delta \le \int_{(-1,1)} g(x)\, dx = \int_{(-1,1)} g_+(x) dx - \int_{(-1,1)} g_-(x)\, dx,$$

which we rewrite as

$$\int_{(-1,1)} g_-(x)\, dx \le 2\delta + \int_{(-1,1)} g_+(x)\, dx.$$

Therefore

$$\int_{(-1,1)} |g|(x)\, dx = \int_{(-1,1)} g_+(x)\, dx + \int_{(-1,1)} g_-(x)\, dx \le 2\delta + 2\int_{(-1,1)} g_+(x)\, dx. \tag{4.17}$$

From (4.16) and $|f_y| = 1$ we have

$$g(x) \le |\partial_1 u| - 1 \le \operatorname{dist}(Du(x,y), K),$$

which implies $g_+(x) \le \operatorname{dist}(Du(x,y), K)$, so that (4.17) becomes

$$\int_{(-1,1)} |g|(x)\, dx \le 2\delta + 2\int_{(-1,1)} \operatorname{dist}(Du, K)(x,y)\, dx.$$

Integrating over $y \in I$ leads to

$$\begin{aligned} \int_S |f_y \cdot (\partial_1 u(x,y) - f_y)|\, dx\, dy &= \int_S |f_y \cdot \partial_1 u(x,y) - 1|\, dx\, dy \\ &\le 2\delta\ell + 2\int_S \operatorname{dist}(Du, K)\, dx\, dy \\ &\le 2\delta\ell + 3\ell E^{1/2}, \end{aligned} \tag{4.18}$$

where in the last step we used Hölder's inequality, $\mathcal{L}^2(S) = 2\ell$, and (4.12).

We now estimate the other component of $\partial_1 u - f_y$, using the same trick as in Lemma 3.3 of Ref. 6. Let $a : S \to S^1$ be a measurable function with $|\partial_1 u - a| \leq \operatorname{dist}(Du, K)$. Using $|a - f_y|^2 = 2 - 2a \cdot f_y = 2f_y \cdot (f_y - a)$ we obtain

$$\begin{aligned}\int_S |a - f_y|^2 \, dx \, dy =& 2 \int_S f_y \cdot (f_y - a) \, dx \, dy \\ \leq& 2 \int_S [f_y \cdot (f_y - \partial_1 u) + \operatorname{dist}(Du, K)] \, dx \, dy \\ \leq& 4\delta\ell + 9\ell E^{1/2},\end{aligned}$$

which leads, using Hölder, $\sqrt{a+b} \leq \sqrt{a} + \sqrt{b}$, (4.12) and then $E \leq 1$, to

$$\begin{aligned}\int_S |\partial_1 u - f_y| \, dx \, dy \leq& \int_S [\operatorname{dist}(Du, K) + |a - f_y|] \, dx \, dy \\ \leq& 3\delta^{1/2}\ell + 3\sqrt{2}\ell E^{1/4} + \sqrt{2}\ell E^{1/2} \leq 3\delta^{1/2}\ell + 6\ell E^{1/4}.\end{aligned} \tag{4.19}$$

Step 3. We obtain a lower bound on $\partial_1(u - u^*)$ *from* (4.14).
We fix a test function $\psi \in C_c^\infty(I; [0, 1])$ such that

$$\frac{1}{2}\ell \leq \int_I \psi(y) \, dy \quad \text{and} \quad |\psi|(y) + \ell|\psi'(y)| + \ell^2|\psi''(y)| \leq c \quad \text{for all } y \in I \tag{4.20}$$

(this is similar to what done in Lemma 3.6 of Ref. 6). We recall that $\partial_2 u^*(x, y) = (1 + \alpha x) f_y^\perp$. Further, from $f_y' = \alpha f_y^\perp$ we obtain $|f_y - f_{y_0}| \leq \alpha\ell$ for all $y \in I$ and therefore

$$|\partial_2 u^*(x_*, y) - (1 + \alpha x_*) f_{y_0}^\perp| = (1 + \alpha x_*)|f_y - f_{y_0}| \leq (1 + \alpha)\alpha\ell \leq \frac{1}{8}\alpha$$

for all $y \in I$, since we chose $\ell \leq 1/16$. Let $F_* \in K$ be the matrix entering (4.14). The vector $(1 + \alpha x_*) f_{y_0}^\perp$ has length $1 + \alpha x_*$; the vector $F_* e_2$ has length either $1 + \alpha$ or $1 - \alpha$. From $x_* \in (-\frac{3}{4}, \frac{3}{4})$ we obtain $|F_* e_2 - \partial_2 u^*(x_*, y_0)| \geq \frac{1}{4}\alpha$, so that there is $b \in S^1$ with

$$\frac{1}{8}\alpha \leq b \cdot (F_* e_2 - \partial_2 u^*(x_*, y)) \qquad \text{for all } y \in I.$$

With (4.14) and (4.20)

$$\begin{aligned}\frac{1}{16}\alpha\ell \leq& \int_I \frac{1}{8}\alpha\psi(y) dy \leq b \cdot \int_I (F_* e_2 - \partial_2 u^*(x_*, y))\psi(y) dy \\ \leq& b \cdot \int_I \partial_2(u - u^*)(x_*, y)\psi(y) dy + c\ell^2\varepsilon^{-1}E + c\ell E^{1/2}.\end{aligned}$$

We compute

$$\begin{aligned}b \cdot \int_I \partial_2(u - u^*)(x_*, y)\psi(y) dy =& - b \cdot \int_I (u - u^*)(x_*, y)\psi'(y) dy \\ \leq& c\delta - b \cdot \int_{(-1, x_*) \times I} \partial_1(u - u^*)(x, y)\psi'(y) \, dx \, dy\end{aligned}$$

where in the second step we used the boundary condition $|u-u^*|(-1,y) \le \delta$, (4.20) and $|b| = 1$. We write $b = -g_1(y)f_y - g_2(y)f_y^\perp$, with $g_1(y) := -b\cdot f_y$, $g_2(y) := -b\cdot f_y^\perp$. Inserting this in the previous expression gives

$$\begin{aligned}\frac{1}{16}\alpha\ell \le & c\big(\delta + \ell^2\varepsilon^{-1}E + \ell E^{1/2}\big) \\ & + \int_{(-1,x_*)\times I} g_1(y) f_y \cdot \partial_1(u-u^*)(x,y)\psi'(y)\,dx\,dy \\ & + \int_{(-1,x_*)\times I} g_2(y) f_y^\perp \cdot \partial_1(u-u^*)(x,y)\psi'(y)\,dx\,dy.\end{aligned}$$

We distinguish three cases, depending on which of the three terms is larger. In case I,

$$\alpha\ell \le c\delta + c\ell^2\varepsilon^{-1}E + c\ell E^{1/2}. \tag{4.21}$$

In case II,

$$\alpha\ell \le c\int_{(-1,x_*)\times I} g_1(y) f_y \cdot \partial_1(u-u^*)(x,y)\psi'(y)\,dx\,dy; \tag{4.22}$$

and in case III,

$$\alpha\ell \le c\int_{(-1,x_*)\times I} g_2(y) f_y^\perp \cdot \partial_1 u(x,y)\psi'(y)\,dx\,dy \tag{4.23}$$

(one term drops since $f_y^\perp \cdot \partial_1 u^* = 0$). The three cases shall be brought together in Step 4.

In case II, recalling (4.20) and $|g| \le 1$,

$$\alpha\ell \le \frac{c}{\ell}\int_{(-1,1)\times I} |f_y \cdot \partial_1(u-u^*)(x,y)|\,dx\,dy; \tag{4.24}$$

and with (4.18) we obtain

$$\alpha\ell \le c\delta + cE^{1/2}. \tag{4.25}$$

Consider now case III. This case is more complex, and is the one leading indeed to the optimal scaling. We proceed as in Lemma 3.6 of Ref. 6. For every $G \in K$ there is $\sigma \in \{\pm 1\}$ such that $(1+\sigma\alpha)Ge_1 = -(Ge_2)^\perp$. For every $(x,y) \in S$ we choose $G \in K$ such that $|Du - G| = \mathrm{dist}(Du, K)$, and observe that

$$\begin{aligned}(\partial_2 u)^\perp &= ((Du-G)e_2)^\perp + (Ge_2)^\perp = ((Du-G)e_2)^\perp - (1+\sigma\alpha)Ge_1 \\ &= ((Du-G)e_2)^\perp + (1+\sigma\alpha)((Du-G)e_1) - \sigma\alpha\partial_1 u - \partial_1 u,\end{aligned}$$

all evaluated at (x,y). Taking the component perpendicular to f_y leads to

$$\begin{aligned}|f_y^\perp \cdot (\partial_1 u + (\partial_2 u)^\perp)| &\le 2|Du-G| + \alpha|f_y^\perp \cdot \partial_1 u| \\ &\le 2\mathrm{dist}(Du,K) + \alpha|\partial_1 u - f_y|.\end{aligned}$$

Therefore (4.23) leads to

$$\begin{aligned}\alpha\ell \leq & c\int_{(-1,x_*)\times I} g_2(y) f_y^\perp \cdot \partial_1 u(x,y)\psi'(y)\,dx\,dy \\ \leq & -c\int_{(-1,x_*)\times I} g_2(y) f_y \cdot \partial_2 u(x,y)\psi'(y)\,dx\,dy \\ & + c\|\psi'\|_{L^\infty}\int_{(-1,x_*)\times I}[2\mathrm{dist}(Du,K)+\alpha|\partial_1 u - f_y|]\,dx\,dy.\end{aligned}$$

We subdivide case III further, depending on which of the two terms is larger. In case (III_A), the second is the largest, and recalling (4.20), (4.12) and (4.19), we obtain

$$\alpha\ell \leq c\|\psi'\|_{L^\infty}\int_S [2\mathrm{dist}(Du,K)+\alpha|\partial_1 u - f_y|]\,dx\,dy \leq \frac{c}{\ell}[\ell E^{1/2} + \alpha\delta^{1/2}\ell + \alpha\ell E^{1/4}]. \tag{4.26}$$

In case (III_B) instead, using $f_y \cdot \partial_2 u^* = 0$, integrating by parts and recalling $f_y' = \alpha f_y^\perp$,

$$\begin{aligned}\frac{1}{c}\alpha\ell \leq & -\int_{(-1,x_*)\times I} \partial_2 u(x,y)\cdot f_y g_2(y)\psi'(y)\,dx\,dy \\ = & -\int_{(-1,x_*)\times I} (\partial_2 u - \partial_2 u^*)(x,y)\cdot f_y g_2(y)\psi'(y)\,dx\,dy \\ = & \int_{(-1,x_*)\times I} (u-u^*)(x,y)\cdot (f_y g_2(y)\psi'(y))'\,dx\,dy \\ = & \int_{(-1,x_*)\times I} (u-u^*)(x,y)\cdot f_y (g_2(y)\psi'(y))'\,dx\,dy \\ & + \int_{(-1,x_*)\times I} (u-u^*)(x,y)\cdot f_y^\perp \alpha g_2(y)\psi'(y)\,dx\,dy.\end{aligned} \tag{4.27}$$

With $|g_2| \leq 1$, $|g_2'| \leq 1$, and (4.20), this reduces to

$$\begin{aligned}\alpha\ell \leq & \frac{c}{\ell^2}\int_S |(u-u^*)(x,y)\cdot f_y|\,dx\,dy \\ & + \frac{c\alpha}{\ell}\int_S |(u-u^*)(x,y)\cdot f_y^\perp|\,dx\,dy.\end{aligned}$$

In each term we use Poincaré's inequality in the x direction and the boundary data to get

$$\begin{aligned}\alpha\ell \leq & c\frac{\delta}{\ell} + \frac{c}{\ell^2}\int_S |f_y\cdot\partial_1(u^*-u)(x,y)|\,dx\,dy \\ & + \frac{c\alpha}{\ell}\int_S |f_y^\perp\cdot\partial_1(u^*-u)(x,y)|\,dx\,dy.\end{aligned}$$

With (4.18) and (4.19),

$$\begin{aligned}\alpha\ell \leq & c\frac{\delta}{\ell} + \frac{c}{\ell^2}[\delta\ell + \ell E^{1/2}] + \frac{c\alpha}{\ell}[\delta^{1/2}\ell + \ell E^{1/4}] \\ & \leq c\frac{\delta}{\ell} + c\alpha\delta^{1/2} + c\frac{1}{\ell}E^{1/2} + c\alpha E^{1/4}.\end{aligned} \tag{4.28}$$

Step 4. Conclusion.
At this point we have shown the existence of a universal constant $c_* > 0$ such that for any choice of $\ell \in (0, \frac{1}{16}]$ one of the following holds. In case I, from (4.21) we have

$$\alpha\ell \leq c_*\delta + c_*\ell^2\varepsilon^{-1}E + c_*\ell E^{1/2}.$$

In case II, from (4.25) we have

$$\alpha\ell \leq c_*\delta + c_*E^{1/2}.$$

In case III_A, from (4.26) we have

$$\alpha\ell \leq c_*\alpha\delta^{1/2} + c_*\alpha E^{1/4} + c_*E^{1/2}.$$

In case III_B, from (4.28) we have

$$\alpha\ell \leq c_*\frac{\delta}{\ell} + c_*\alpha\delta^{1/2} + c_*\frac{1}{\ell}E^{1/2} + c_*\alpha E^{1/4}.$$

It remains to choose ℓ. We assume that

$$c_*\delta \leq \frac{1}{3}\alpha\ell^2 \quad \text{and} \quad c_*\delta^{1/2} \leq \frac{1}{3}\ell, \tag{4.29}$$

so that all δ-dependent terms in the above equations can be absorbed in the left-hand side. We remark that the first condition is the most stringent one for small α. Then the four cases above can be summarized in the estimate

$$E \geq c\min\{\frac{\alpha\varepsilon}{\ell}, \alpha^2, \alpha^2\ell^2, \alpha^2\ell^4, \ell^4\} = c\min\{\frac{\alpha\varepsilon}{\ell}, \alpha^2\ell^4\}$$

where we eliminated irrelevant terms using $\alpha \leq 1$ and $\ell \leq 1$. We finally set $\ell := \frac{1}{16}(\varepsilon/\alpha)^{1/5}$, and obtain $E \geq c\alpha^{6/5}\varepsilon^{4/5}$. If the constant c_1 in the statement is chosen appropriately (depending only on c_*) then the assumption $\delta \leq c_1\alpha^{3/5}\varepsilon^{2/5}$ implies (4.29). □

4.2. *The lower bound in Theorem 2.3*

Lemma 4.4. *For any $m \geq 1$ there exists $c_m > 0$ such that for any $\alpha \in (0, \frac{1}{2}]$, $\varepsilon \in (0, \alpha]$, and $u \in S_{\mathrm{ex}} \cap S^{(m)}_{\mathrm{onescale}}$ we have*

$$E_\varepsilon[u] \geq c_m\alpha^{5/4}\varepsilon^{3/4}.$$

Proof. Let $u \in S_{\mathrm{ex}} \cap S^{(m)}_{\mathrm{onescale}}$ as in the statement, $h \in (0, 1]$ be as in the definition of $S^{(m)}_{\mathrm{onescale}}$, and $E := E_\varepsilon[u]$. For $y_0 \in (-1, 1-h)$ we consider the square $Q^h(y_0) :=$

$(1-h,1)\times(y_0,y_0+h)$ as in Definition 2.2. We consider the set $G_+^{m,h}$ of the $y\in(-1,1-h)$ such that u has no microstructure in $Q^h(y_0)$, defined in (2.21). Using Fubini's theorem we estimate

$$\int_{G_+^{m,h}}\int_{Q^h(y_0)}\operatorname{dist}^2(Du,K)\,dx\,dy\,dy_0\le h\int_{(1-h,1)\times(-1,1)}\operatorname{dist}^2(Du,K)\,dx\,dy\le hE.$$

Since by assumption $\mathcal{L}^1(G_+^{m,h})\ge\frac{1}{m}$ we can choose $y_0\in G_+^{m,h}$ (fixed for the rest of the proof) such that

$$\int_Q\operatorname{dist}^2(Du(x,y),K)\,dx\,dy\le mhE,$$

where for brevity we write $Q:=Q^h(y_0)$. By the definition of $G_+^{m,h}$ there is $J\in\{A,B\}$ such that

$$\int_Q\operatorname{dist}^2(Du,\mathrm{SO}(2)J)\,dx\,dy\le m\int_Q\operatorname{dist}^2(Du,K)\,dx\,dy.$$

We are now in position to apply the geometric rigidity estimate in Th. 3.1 of Ref. 16 to the function $u\circ J^{-1}$ on the set JQ and conclude that there exists $R\in\mathrm{SO}(2)$ such that

$$\int_Q|Du-RJ|^2\,dx\,dy\le c\int_Q\operatorname{dist}^2(Du,\mathrm{SO}(2)J)\,dx\,dy\le chE$$

with a constant $c=c(m)$ (from now on all constants may depend implicitly on m). By Poincaré's inequality and the trace theorem, there exists $b\in\mathbb{R}^2$ such that, with $F:=RJ\in K$,

$$\int_{\partial Q}\left|u-F\begin{pmatrix}x\\y\end{pmatrix}-b\right|^2d\mathcal{H}^1(x,y)\le ch\int_Q|Du-F|^2\,dx\,dy\le ch^2E.$$

But since $u(1,y)=\frac{1+\alpha}{\alpha}f_y$, we have

$$\int_0^h\left|\frac{1+\alpha}{\alpha}\begin{pmatrix}\cos(\alpha(t+y_0))\\\sin(\alpha(t+y_0))\end{pmatrix}-b-F\begin{pmatrix}1\\t+y_0\end{pmatrix}\right|^2dt\le ch^2E.$$

On the other hand,

$$\begin{aligned}\min_{b\in\mathbb{R}^2}\min_{F\in\mathbb{R}^{2\times2}}\min_{y\in\mathbb{R}}\int_0^h\left|\frac{1+\alpha}{\alpha}\begin{pmatrix}\cos(\alpha(t+y))\\\sin(\alpha(t+y))\end{pmatrix}-b-F\begin{pmatrix}1\\(t+y)\end{pmatrix}\right|^2dt\\ \ge C\int_0^h\alpha^2t^4dt=C\alpha^2h^5.\end{aligned}\tag{4.30}$$

(The inequality (4.30) can be proved by passing to complex notation. Since $e^{i\alpha(t+y)}=e^{i\alpha t}e^{i\alpha y}$ and $|e^{i\alpha y}|=1$, the result for general y is easily reduced to the case $y=0$. One is then left to estimate how well $\frac{\alpha}{1+\alpha}e^{i\alpha t}$ can be estimated in

$L^2(0,h)$ by an affine function. The answer is driven by the quadratic term in its Taylor expansion.) Altogether, we have

$$C\alpha^2 h^5 \le h^2 E$$

which is the same as $E \ge C\alpha^2 h^3$. On the other hand, the condition (2.22) implies $E \ge \frac{c\varepsilon\alpha}{h}$. Combining these two lower bounds, we get the desired bound

$$E \ge c \min_{h'>0} \max\{\alpha^2 (h')^3, \frac{\alpha\varepsilon}{h'}\} = c\alpha^{5/4}\varepsilon^{3/4}.$$

where the latter infimum is attained at $h' = (\varepsilon/\alpha)^{1/4}$. □

Acknowledgments

This work was partially supported by the Deutsche Forschungsgemeinschaft through project 211504053/SFB1060 and project 441211072/SPP2256, and by the National Science Foundation through grants 0967140, 1311833, and 2009746. The research of Oleksandr Misiats was supported by Simons Foundation - Collaboration Grant for Mathematicians no. 854856.

References

1. J. M. Ball and R. D. James, Fine phase mixtures as minimizers of energy, *Archive for Rational Mechanics and Analysis* **100** (1987) 13–52.
2. J. M. Ball and R. D. James, Proposed experimental tests of a theory of fine microstructure and the two-well problem, *Philosophical Transactions of the Royal Society of London. Series A: Physical and Engineering Sciences* **338** (1992) 389–450.
3. Z. S. Basinski and J. W. Christian, Crystallography of deformation by twin boundary movements in indium-thallium alloys, *Acta Metallurgica* **2** (1954) 101–116.
4. K. Bhattacharya, *Microstructure of martensite: Why it forms and how it gives rise to the shape-memory effect* (Oxford University Press, 2004).
5. A. Chan and S. Conti, Energy scaling and domain branching in solid-solid phase transitions, in *Singular phenomena and scaling in mathematical models* (Springer, Cham, 2014), pp. 243–260.
6. A. Chan and S. Conti, Energy scaling and branched microstructures in a model for shape-memory alloys with SO(2) invariance, *Mathematical Models and Methods in Applied Sciences* **25** (2015) 1091–1124.
7. H. D. Chopra, C. Bailly and M. Wuttig, Domain structures in bent In-22.5 at.% Tl polydomain crystals, *Acta Materialia* **44** (1996) 747–751.
8. H. D. Chopra, A. L. Roytburd and M. Wuttig, Temperature-dependent deformation of polydomain phases in an In-22.5 at. pct Tl shape memory alloy, *Metallurgical and Materials Transactions A* **27** (1996) 1695–1700.
9. R. Chulist, L. Straka, H. Seiner, A. Sozinov, N. Schell and T. Tokarski, Branching of (110) twin boundaries in five-layered Ni-Mn-Ga bent single crystals, *Materials and Design* **171**.
10. L. Collins and K. Bhattacharya, Optimal design of a model energy conversion device, *Structural and Multidisciplinary Optimization* **59** (2019) 389–401.
11. S. Conti, Branched microstructures: scaling and asymptotic self-similarity, *Communications on Pure and Applied Mathematics* **53** (2000) 1448–1474.

12. S. Conti, J. Diermeier, D. Melching and B. Zwicknagl, Energy scaling laws for geometrically linear elasticity models for microstructures in shape memory alloys, *ESAIM: COCV* **26** (2020) 115.
13. S. Conti, R. V. Kohn and O. Misiats, An energy minimization approach to twinning with variable volume fraction, In preparation.
14. B. Dacorogna, *Direct methods in the calculus of variations*, volume 78 of *Applied Mathematical Sciences* (Springer, New York, 2008), second edition.
15. R. B. Flippen and C. W. Haas, Nonplanar domain walls in ferroelastic $Gd_2(MoO_4)_3$ and $Pb_3(PO_4)_2$, *Solid State Communications* **13** (1973) 1207–1209.
16. G. Friesecke, R. D. James and S. Müller, A theorem on geometric rigidity and the derivation of nonlinear plate theory from three-dimensional elasticity, *Communications on Pure and Applied Mathematics* **55** (2002) 1461–1506.
17. Y. Ganor, T. Dumitrică, F. Feng and R. D. James, Zig-zag twins and helical phase transformations, *Philosophical Transactions of the Royal Society A: Mathematical, Physical and Engineering Sciences* **374**.
18. F. Jouve, Structural shape and topology optimization, in *Topology Optimization in Structural and Continuum Mechanics*, eds. G. I. N. Rozvany and T. Lewiński (Springer Vienna, Vienna, 2014), pp. 129–173.
19. A. Khachaturyan, *Theory of Structural Transformations in Solids* (Wiley, New York, 1983), reprinted by Dover Publications, Mineola, NY in 2008.
20. R. V. Kohn, Energy-driven pattern formation, in *International Congress of Mathematicians. Vol. I* (Eur. Math. Soc., Zürich, 2007), pp. 359–383.
21. R. V. Kohn and S. Müller, Branching of twins near an austenite—twinned-martensite interface, *Philosophical Magazine A* **66** (1992) 697–715.
22. R. V. Kohn and S. Müller, Relaxation and regularization of nonconvex variational problems, *Rendiconti del Seminario Matematico e Fisico di Milano* **62** (1992) 89–113.
23. R. V. Kohn and S. Müller, Surface energy and microstructure in coherent phase transitions, *Communications on Pure and Applied Mathematics* **47** (1994) 405–435.
24. R. V. Kohn, S. Müller and O. Misiats, A scalar model of twinning with variable volume fraction: global and local energy scaling laws, In preparation.
25. R. V. Kohn and F. Otto, Small surface energy, coarse-graining, and selection of microstructure, *Physica D: Nonlinear Phenomena* **107** (1997) 272–289, 16th Annual International Conference of the Center for Nonlinear Studies.
26. A. Kuroda, K. Ozawa, Y. Uesu and Y. Yamada, Simulation study of zigzag domain boundary formation in ferroelectric-ferroelastics using the TDGL equation, *Ferroelectrics* **219** (1998) 215–224.
27. S. Meeks and B. Auld, Periodic domain walls and ferroelastic bubbles in neodymium pentaphosphate, *Applied Physics Letters* **47** (1985) 102–104.
28. S. Müller, Variational models for microstructure and phase transitions, in *Calculus of variations and geometric evolution problems (Cetraro, 1996)*, eds. F. Bethuel, G. Huisken, S. Müller, K. Steffen, S. Hildebrandt and M. Struwe (Springer, Berlin, 1999), volume 1713 of *Lecture Notes in Mathematics*, pp. 85–210.
29. A. L. Roitburd, Martensitic transformation as a typical phase transformation in solids, (Academic Press, 1978), volume 33 of *Solid State Physics*, pp. 317–390.
30. A. L. Roitburd, Instability of boundary regions and formation of zigzag interdomain and interfacial walls, *Journal of Experimental and Theoretical Physics Letters* **47** (1988) 171–174.
31. A. L. Roitburd, M. Wuttig and I. Zhukovskiy, Non-local elasticity of polydomain phases, *Scripta Metallurgica et Materialia* **27** (1992) 1343–1347.